REVIEWS OF MODERN PHYSICS VOLUME 31, NUMBER 4 OCTOBER, 1959

Interaction of Normal Modes with Electron Traps

JORDAN J. MARKHAM

Research Department, Zenith Radio Corporation, Chicago, Illinois

1. INTRODUCTION

CONSIDER an electron trap in a solid with two levels, *u* (upper) and *g* (ground). A fundamental question is: how does an electron transition affect the normal vibrational modes of the crystal? The answer so far has been obtained either with the use of a phenomenological macroscopic theory, or by the use of configurational coordinate curves.

The phenomenological theory, due to Fröhlich (F1,* F2, and H4; also Born and Huang, B2, p. 82), ignores details of the lattice structure. In a polar crystal Fröhlich assumes that the forces on the ions, as well as the polarization, depend exclusively on the macroscopic electric field and relative ionic displacements at the point in question. This model leads to pure transverse and longitudinal modes. It is only true for the longest "optical" waves in which the positive and negative ions vibrate 180° out of phase. This theory does not account for the change in the character of the normal mode with decreasing wavelength. In NaCl the longitudinal optical branch in certain directions has a frequency drop of 57%, and the shortest waves are pure acoustical, in which the ions vibrate in phase (M3). Fröhlich's model is useful in the theory of reststrahlen where one deals with electromagnetic radiations whose wavelength is large compared to the inter-ionic distances, but this approach is questionable for phenomena which depend critically on short range effects.

The configurational coordinate model assumes that a very small number of local modes surround a point imperfection. This approach is supported by recent calculations. (See M2 and references therein.) One would expect the local modes to have frequencies in the gap between the acoustical and optical branches. This suggests that their frequency spread may be small. We refer to this model by the letters LM. It is assumed that there are one or several "effective" frequencies associated with the local modes. The extreme situation where there is only one mode is referred to by the letters CC (configuration coordinate, D1). The LM models cannot give a completely correct picture since long range effects must exist in polar solids. The Fröhlich model cannot either, since it ignores local lattice distortions.

One of the most important effects of the electron-phonon interaction is the broadening of optical absorption lines. Studies of these phenomena will give information regarding the effects of electronic transitions on normal modes.

In general, rigorous quantum mechanics has been used on this problem when the phenomenological model is employed. The original techniques required infinitely small interaction between the trapped electron and the modes. It, therefore, could not be used in the LM or CC models.

While these developments were taking place, Williams (W2), as well as Williams and Hebb (W3), developed

---

* Refer to items in the Bibliography at the end of the paper.

an independent treatment which was applied to the CC model. This approach makes a series of approximations and is sometimes referred to as "semiclassical." A more detailed justification of Williams' method has been made by Lax (L1), Klick (K2), and Dexter (D1). This development shows that at very low temperatures the shape of an absorption band should be Gaussian (provided that the electronic transition does not induce a frequency change in the CC mode). Further, the position of maximum absorption is temperature independent even if the frequency changes.

Since 1950 the rigorous quantum mechanical method has been fully developed, and one can now apply it to various LM models. Williams' simpler approach is still very useful, since it gives a vivid picture of the absorption process. However, it is beset by many approximations, and the final results do not always agree with more rigorous calculations.

To summarize the development so far, we have several models—phenomenological (Fröhlich), local modes, and configurational coordinate. We have two means of calculating shapes of bands—Williams', and the rigorous quantum mechanical approach. For some models the second method can be carried through in detail. Most realistic ones, however, require Williams' approach. A rather formal theory for all models has been worked out by Kubo and Toyozawa (K6).

This paper attempts to synthesize the rigorous theory and to apply it to various models. We start by examining the Hamiltonian to be used (Part I). Fortunately, it can be written in a form that applies to all the models. We next discuss the properties of these Hamiltonians and point out the essential difference between phonon-electron and photon-electron interactions. Only in special types of solid state problems may they be considered similar. At this stage, one can see why multiphonon processes occur. Some of the results of Part I are known, but their interrelations have not been fully understood. This has led to appreciable confusion. Some of the mathematical techniques are those used by Born and Huang in connection with another problem.

After this development, the photon absorption problem is considered rigorously and in some detail (Part II). The Hamiltonian developed permits a unification of the field which is most desirable, since experimental results are being obtained.

Applications of the theory are not considered because the author does not trust the presently available data. The absorption band associated with the *F* center in KCl has been measured a great many times. It seems to fulfill the requirement stated in the first paragraph. Various laboratories, however, do not report the same results. A typical set of half-width, *H*, measurements are shown in Table I.†

TABLE I. *H* of KCl.

θ (°K)	*H* (ev)	Observer
28	0.19	Mollow (M10)
4	0.18	Russell and Klick (R1)
4	0.17	Burstein and Oberly (B5)
5	0.168	Compton and Klick (C3)
5	0.17	Duerig and Markham (D2)
5	0.163	Markham and Konitzer (M4)
85 (App)	0.26	Molnar (M11)
87	0.23	Mollwo (M10)
87	0.243	Kanzaki (K1)
77	0.3	van Doorn and Haven (D3)
77	0.22	Russell and Klick (R1)
77	0.20	Burstein and Oberly (B5)
78	0.20	Duerig and Markham (D2)
78	0.193	Konitzer and Markham (K4)
77	0.196	Compton (C2)

At low temperatures *H* can be measured to about five parts per thousand so that the variations cannot be attributed to experimental error (M1). The author doubts that the scatter is related to the sample purity, and the temperature variation of *H* is too small to explain the discrepancies. Experiments have shown (K3) that, unless special care is taken, any values between 0.19 ev and 0.25 ev can be obtained for *H* (in KCl at 78°K). Improper quenching and very slight exposure to light produce new bands, and *H* then corresponds to a composite.

Although not comparing the results with experiment, an attempt is made to present the argument in such a manner that a comparison with data is readily possible. Indeed, a comparison has been made with recent data on the *F* center in KCl. The agreement on the whole is satisfactory. It is hoped that in the next few years sufficient experimental data will become available to justify and amplify the theory presented here.

The first theory of the shape of an absorption band in a solid is due to Smakula (S2), who assumed that a trapped electron behaves like a damped oscillator in a dielectric medium. Nothing in this theory explains the temperature dependence of the damping term. The first attempt to associate the width theoretically with the thermal vibration was done independently by Muto (M13), by Huang and Rhys (H5), and by Pekar (P1) (also P2, 3, and 4). Huang-Rhys and Pekar used Fröhlich's model and assumed that the electron interacts only an infinitesimally small amount with all the longitudinal optical modes. Thus they limited themselves to first order terms in the various expansions, as did Muto.

Pekar obtained two expressions for the shape; it should be nonsymmetric at low temperatures but Gaussian at high temperatures. He employed the reststrahlen frequency combined with the Lyddane-Sacks-Teller (LST) relation to determine the longitudinal frequency (B2, p. 82–128). He also made a comparison of his theory with Mollwo's data (M10).

O'Rourke (O1) made a fundamental extension of the previous calculations, eliminating the restriction that

---

† Half-width is defined in Appendix I.

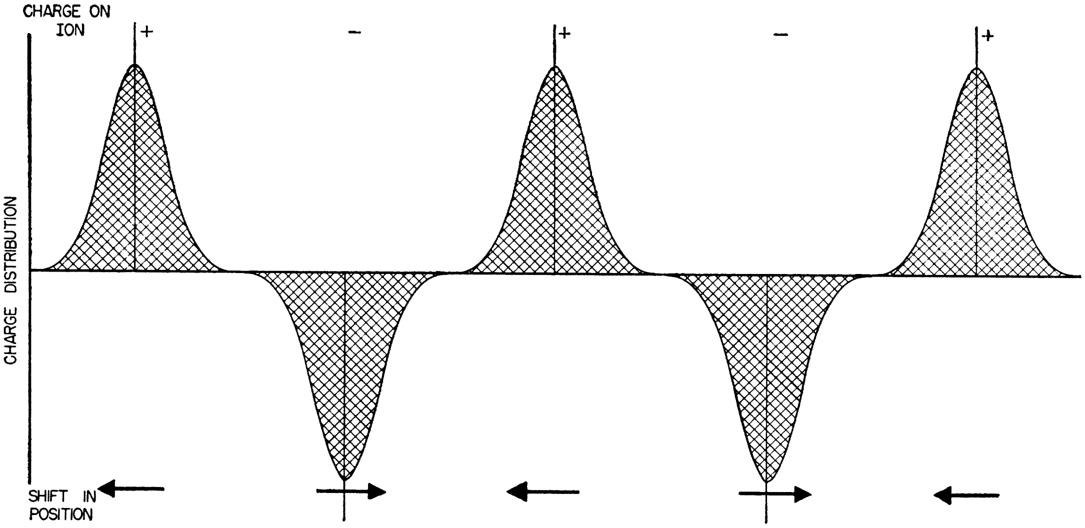

FIG. 1. Schematic diagram showing the effects of trapping an electron at an imperfection.

the electron-phonon interaction must be infinitely small. His most general expressions are limited by the assumption that electronic transitions do not cause frequency changes. To use his expressions one must assume that a single "effective" vibrational frequency exists. His results apply to the Fröhlich Hamiltonian, the CC model, as well as to an LM model, if a single effective frequency exists. Pekar's expansions may therefore be combined with the CC or LM model to calculate the shape rigorously at very low temperatures. We do this and show that the shape is not the one predicted on the basis of the Williams' approximation. Present low-temperature data indicate that the more rigorous treatment is correct.

At about the same time, Lax (L2) developed some completely general relations between the moment of the distribution and the temperature. Meyer (M8 and 9) extended the development of Lax, giving a general approach to the problem. This method is not limited to Fröhlich's Hamiltonian which was employed by Meyer. For the calculation to be valid, it is necessary to use an orthogonal set of eigenfunctions. We show here that this is true. Further, we indicate that Meyer omits some important terms.

Meyer also made a serious attempt to analyze Mollwo's data by means of the new theories. His results are most impressive and by themselves give a good proof of the reliability of his calculation and a validity of the LST relation. This is not confirmed by more recent measurements (see Table I). The method of analysis to be employed is of fundamental importance. An alternate analysis of Mollwo's data indicates that the effective frequency is 3.2×10^{12} sec^{-1} for KCl. The LST relation gives 6.3×10^{12} sec^{-1}. This difference suggests that Fröhlich's model does not apply to the *F* center in KCl. Other analyses (R1, K4) support this view. The means of analysis is the important difference between Meyer's conclusion and those obtained recently.

This field has been reviewed by Pekar (P3, P4), Lax (L2), Meyer (M9), Klick and Schulman (K2a), and Dexter (D1). Pekar's reviews, though out of date, are extremely important contributions to the field. Lax's review concerns itself primarily, though not entirely, with Williams' approximation. Meyer's review is limited to Fröhlich's model and omits some important developments made by Pekar. Klick and Schulman consider only Williams' approach. Dexter considered both aspects of the problem, applying the quantum mechanical treatment to Fröhlich's model and Williams' approximation to the CC model.

This paper concentrates on the pure quantum mechanical approach and treats all models. Some aspects of the problem are considered in greater detail than has been done previously. These aspects are most important since they can be checked experimentally.

The theory is not developed in full; instead, results are quoted from the recent book of Born and Huang (B2), which is cited by the letter B. Those parts of the theory which have not been presented in book or review article form are more fully discussed. Although the theory applies to any imperfection with two or more bound states, the development is closely related to the *F* center, since this has been studied in greatest detail.

Part I. The Hamiltonian

2. PHYSICAL CONCEPTS INVOLVED IN ELECTRON-PHONON INTERACTIONS

The trapping of an electron at a site has three effects. These can be intuitively understood by means of Fig. 1, which is a schematic representation of the nuclei (shielded by the inner electrons) for a one-dimensional polar crystal.

The nuclei of the solid are assumed to be initially distributed uniformly. When an electron is trapped nearby (to the left of the diagram) the following effects occur.

(1) The electron induces a force on the nuclei, causing a nonuniform shift of the rest positions, as indicated by the arrows. This action is very much like a compression (or expansion) of a spring and leads to the storing of energy.

(2) The forces between the nuclei are slightly modified, leading to a shift in the angular frequencies of the lattice, $\Delta\omega$. At absolute zero the probable position of an ion is given by a Gaussian curve if an Einsteinian model is used (no coupling between ions). The trapping causes a broadening or narrowing of the distribution. The Einsteinian solid is used here only to illustrate the effect.

(3) Finally, there is a third effect similar to a photon-electron interaction—the electron's self-energy. The electrons and nuclei readjust their probable distributions so that the total energy is at a minimum. This effect may be visualized by means of time dependent perturbation theory leading to electron-phonon transitions, or by time independent perturbation theory (or even variational methods) leading to wave functions which are no longer single products of electronic and nuclear wave functions. This is referred to as the electron-nuclear correlation.

These effects also occur when an electron redistributes itself, i.e., acquires a new wave function by jumping from one bound state to another, or by transitions to the conduction band. Item (3) is similar to phenomena which occur in electrodynamics, while (1) and (2) arise in systems made of light and heavy particles. The relative importance of these effects depends on the forces within the solid. In many solids, effects (1) and (2) are so small that phonon-electron interaction problems resemble problems in electrodynamics. This is true in metals and in some semiconductors. In general, the phonon-electron problem has a different character because of effects (1) and (2). Our interest here is the difference between phonon-electron and photon-electron interactions; hence, effect (3) is not considered in detail. Usually the effects are considered independently.

Treatments of the correlation problem appear several places and take various forms. Born and Huang (B, p. 166) considered it briefly in a general manner, while Haken (H1) studied its effect in a special one-dimensional model.

Simpson (S3) and Pekar (P3) considered effect (1) in their calculations on the F center. Williams (W2) in an ambitious and detailed study calculated the displacements which occur when a Tl^+ ion replaces a K^+ ion in a KCl lattice. Williams finds a change in the second derivative of his CC plots which is related to $\Delta\omega$. Klick and Schulman (K2a) have attempted to compute $\Delta\omega$ from experimental data.

The idea of a large frequency shift was invoked by Seitz (S1) to explain the observations of Dutton and Maurer (D4). They measured a thermal activation energy for the V_1 band in KBr of 0.23 ev compared to an optical activation energy of 3.0 ev. These ideas have some theoretical difficulties. A similar problem exists for the F' center whose optical activation energy in KBr is 1.3 ev compared to a thermal activation energy of 0.29 ev (D4).

A problem which involves all three effects is an electron at the bottom of the conduction band in a polar solid. The electron interacts strongly with the surrounding ions. Due to the large difference in the velocity of the electrons and the nuclei, the forces on the nuclei depend on the average distribution of the electron, thus the electron displaces the surrounding ions. This causes effects (1) and (2) and results in a potential well. The well in turn traps the electron. The electron will also be influenced by the polar modes of vibration about the well. This is similar to the interaction between an electron and the zero-point electromagnetic vibrations. The presence of the well may be referred to as self-trapping,‡ while the electron-phonon interaction may be called the polaron effect. In reality, they cannot be separated, although at present the connection between the two is not completely clear.

3. FORMAL THEORY

The complete Hamiltonian for a solid of unit volume is

$$H=T_e+T+V(\mathbf{R}). \qquad (3.1)$$

Here T_e is the kinetic energy operator for all the electrons, T is the kinetic energy operator for the N nuclei, and V is the total potential energy of the system. V depends on the position of all the electrons (denoted by $\mathbf{r}$ when explicitly stated) and all the nuclei (denoted by $\mathbf{R}$). We include in V implicitly any point imperfection such as a missing ion. The notation of (B) will be used, namely, the coordinate of a nucleus is $X_\alpha(k)$ ($\alpha=1, 2, 3$ and $k=1, 2\cdots N$). The explicit expression for T is

$$T=-(\hbar^2/2)\sum_k (1/M_k)\nabla_k^2, \qquad (3.2)$$

where all the nuclei need not have the same mass, M_k.

The Born-Oppenheimer technique assumes that for a fixed value of $\mathbf{R}$ the eigenfunctions, $\varphi_n(\mathbf{R})$, and eigenvalues, $\epsilon_n(\mathbf{R})$, associated with the operator

$$h_e(\mathbf{R})=T_e+V(\mathbf{R}) \qquad (3.3)$$

are known.

---

‡ The assumption has been made that the self-trapping concept implies a stationary distortion of the lattice. There is no reason for this assumption. Indeed, Seitz and the author (M6) suggested at an early date that a self-trapped electron might move through the lattice. The work of Castner and Kanzig (C1) implies that a self-trapped hole has relatively little mobility.

Next, one uses the Hamiltonian

$$h_v(\mathbf{R}_n)=T+\epsilon_n(\mathbf{R})-\epsilon_n(\mathbf{R}_n) \tag{3.4}$$

to obtain a second set of eigenfunctions χ and eigenvalues ϵ_v. The point $\mathbf{R}_n$ of (3.4) is defined by the relations

$$[\partial\epsilon_n/\partial X_\alpha(k)]_{\mathbf{R}_n}=0. \tag{3.4a}$$

To terms in $[\Delta X_\alpha(k)]^3$ we may write (3.4) in the form

$$h_v=T+\tfrac{1}{2}\sum_{\alpha,\beta,k,l}\left[\frac{\partial^2\epsilon_n}{\partial X_\alpha(k)\partial X_\beta(l)}\right]_{\mathbf{R}_n}\Delta X_\alpha(k)\Delta X_\beta(l). \tag{3.5}$$

Here $\Delta X_\alpha(k)$ is the displacement relative to $\mathbf{R}_n$. One may introduce normal coordinates into (3.5) (B, p. 173) which are linear functions of the $\Delta X_\alpha(k)$. The result is

$$h_v=\tfrac{1}{2}\sum_j(p_j^2+\omega_j^2q_j^2), \tag{3.6}$$

where

$$p_j=(\hbar/i)(\partial/\partial q_j), \tag{3.6a}$$

and j goes from 1 to 3 N. The q's have the dimension of length times $(\text{mass})^{\frac{1}{2}}$ and the ω's are given by the secular determinant,

$$\left|\frac{1}{(M_kM_l)^{\frac{1}{2}}}\left[\frac{\partial^2\epsilon_n}{\partial X_\alpha(k)\partial X_\beta(l)}\right]_{\mathbf{R}_n}-\omega^2\delta_{\alpha\beta}\delta_{kl}\right|=0. \tag{3.7}$$

Here δ is the Kronecker delta.

The individual term in (3.6) corresponds to a simple harmonic oscillator with an eigenfunction, χ_{nj}, and an eigenvalue, $\hbar\omega_j(v_j+\frac{1}{2})$. The eigenfunctions associated with h_v are products of such functions and are denoted by χ_n. n corresponds to an electronic state and appears through the use of $\epsilon_n(\mathbf{R})$, and v_j is the vibrational quantum number of the jth mode. v_t is the sum of the v_j's. Since we are mainly concerned with two states, n will at times be replaced by g (ground) and u (upper). Usually the subscript n will not be required. φ and χ will be used for the ground state while φ' and χ' will be employed for the excited state.

To complete the notation, the following definitions are made:

$$\langle\varphi_{n'}|\mathbf{O}|\varphi_n\rangle=\int\varphi_{n'}{}^*\mathbf{O}\varphi_n d\tau, \tag{3.8}$$

where the integration is over all positions of the electrons, and

$$\{\chi_{n'}|\mathbf{O}|\chi_n\}=\int\chi_{n'v'}{}^*\mathbf{O}\chi_{nv}d\mathbf{R}, \tag{3.9}$$

where the integration is over all positions of the nuclei. $\mathbf{O}$ is any operator. It will be omitted when $\mathbf{O}=1$.

The essential problem is to find approximate eigenfunctions for the total Hamiltonian (3.1). By using the foregoing equations, we may define two approximations:

$$(1)\ \text{the static—}\Psi(S)=\varphi(\mathbf{R}_n)\chi \tag{3.10}$$

or

$$(2)\ \text{the adiabatic—}\Psi(A)=\varphi(\mathbf{R})\chi. \tag{3.11}$$

Neither (3.10) nor (3.11) is a complete solution of (3.1). For some problems one desires to split H into a zeroth-order Hamiltonian and a residual which represents a small perturbation. The way this is done depends on the form of Ψ employed.

For the static approximation

$$H_0(S)=h_e(\mathbf{R}_n)+h_v(\mathbf{R}_n) \tag{3.12a}$$

$$H_1(S)=V(\mathbf{R})-V(\mathbf{R}_n)-\tfrac{1}{2}\sum_{\alpha,\beta,k,l}\left[\frac{\partial^2\epsilon_n}{\partial X_\alpha(k)\partial X_\beta(l)}\right]_{\mathbf{R}_n}\Delta X_\alpha(k)\Delta X_\beta(l). \tag{3.12b}$$

On the other hand, in the adiabatic approximation,

$$H_0(A)\varphi(\mathbf{R})\chi=\chi h_e(\mathbf{R})\varphi(\mathbf{R})+\varphi(\mathbf{R})T\chi \tag{3.13a}$$

$$H_1(A)\varphi(\mathbf{R})\chi=-\frac{\hbar^2}{2}\sum_k\left[\frac{2}{M_k}\nabla_k\varphi\cdot\nabla_k\chi+\frac{1}{M_k}\chi\nabla_k{}^2\varphi(\mathbf{R})\right]. \tag{3.13b}$$

$H_0(A)$ assumes that $\varphi(\mathbf{R})$ permutes with T.

An elegant method of arriving at (3.12) was given many years ago by Born and Oppenheimer (B3). This treatment is reproduced in a simpler form by (B, pp. 166–173), who have also found a systematic way to obtain the adiabatic approximation. In the latter case, the χ's contain higher-order anharmonic terms. The Born-Oppenheimer technique involves several steps. Equation (3.4a) is a particularly important one, since it is involved in h_v. Limitations on this technique are discussed in Sec. 5(b).

To obtain the eigenvalues of (3.13a) we may proceed as follows:

$$\begin{aligned}H_0(A)\varphi(\mathbf{R})\chi&=\varphi(\mathbf{R})[\epsilon_n(\mathbf{R})+T]\chi\\&=\varphi(\mathbf{R})[\epsilon_n(\mathbf{R}_n)+h_v]\chi\\&=[\epsilon_n(\mathbf{R}_n)+\epsilon_v]\varphi(\mathbf{R})\chi,\end{aligned} \tag{3.14a}$$

where (3.4a) and (3.5) have been used. The eigenvalues $H_0(S)$ and $H_0(A)$ are equal since

$$H_0(S)\varphi(\mathbf{R}_n)\chi=[\epsilon_n(\mathbf{R}_n)+\epsilon_v]\varphi(\mathbf{R}_n)\chi. \tag{3.14b}$$

In view of (3.14a) and (3.14b) we define the total energy of the system as $E_{nv}=\epsilon_n(\mathbf{R}_n)+\epsilon_v$. We shall again omit the subscripts, using E and E'.

The method of splitting H into parts is based on a physical intuition and the fact that the nuclear mass is much heavier than the electron mass. Mathematically, the splitting has an unfortunate aspect, since some of the nicest mathematical properties do not hold for the H_0's.

One may show (M4) that (1) the static eigenfunctions do not form an orthogonal complete set while (2) the adiabatic eigenfunctions form an orthogonal set with respect to $\mathbf{r}$ and $\mathbf{R}$ space.

The latter can be shown by noting that the $\varphi(\mathbf{R})$'s form a complete set of functions in $\mathbf{r}$ space for a fixed $\mathbf{R}$, and that the χ's form a complete set in $\mathbf{R}$ space for a fixed n. Further, we note

$$\{\langle\varphi_{n'}(\mathbf{R})\chi_{n'v'}|\varphi_n(\mathbf{R})\chi_{nv}\rangle\}=\{\chi_{n'v'}\langle\varphi_{n'}(\mathbf{R})|\varphi_n(\mathbf{R})\rangle\chi_{nv}\}$$
$$=\{\chi_{n'v'}|\delta_{nn'}|\chi_{nv}\}=\delta_{nn'}\delta_{vv'}. \quad (3.15)$$

(3) It can be shown that (B, p. 189)

$$\left[\frac{\partial\epsilon_n}{\partial X_\alpha(k)}\right]_{\mathbf{R}_n}=\left\langle\varphi_n(\mathbf{R}_n)\left|\left[\frac{\partial V}{\partial X_\alpha(k)}\right]_{\mathbf{R}_n}\right|\varphi_n(\mathbf{R}_n)\right\rangle \quad (3.16)$$

(Feynman's Theorem).

For a perfect ionic crystal the lowest eigenvalue of h_e is the total interionic potential, i.e., the coulombic, repulsive, and high-order terms, from which one determines the normal modes by well-developed methods. In the case of interest, all cells in our solid are not equivalent, since there is a point imperfection. In the case of the F center there is a missing negative ion with a trapped electron. Mazur, Montroll, and Potts (M2) have shown that the modes for such a crystal are not identical to those of a perfect lattice. A missing ion creates local modes surrounding the imperfection. These are the vibrations of greatest interest to our problem. In a general way the motion of the ion right around an imperfection is determined primarily by the local modes (Bjork, B1). The object here is not to describe these modes in detail but to indicate what effects electron transitions have on them. The exact relation between local and crystal modes is an extremely complex problem. One of the best ways to study the local modes is to measure their frequencies indirectly. This can be done from measurements of the thermal broadening of absorption and emission bands (Part II).

(a) Ground State

The development so far is completely general. We now use this development for a crystal with an electron trap. Assume that there are two (or more) bound states. Every state generates its own ϵ_n, ω_j's, and q_j's. We start the calculation by using the values appropriate for the ground state. To stress this point we write ϵ_g for ϵ_n; $\omega_j(g)$ for ω_j; $h_v(g)$ for h_v, etc. We shall retain the notation q_j and p_j, however.

(b) Upper State

We could make all the equations apply to the upper state by simply replacing the subscript g by u. The p's and q's of (3.6), however, will be different. The object is to find relations between the two sets; hence, we proceed in a different manner. In this case, the eigenvalue of h_e is $\epsilon_u(\mathbf{R})$ and the trapping energy may be defined as

$$\Delta\epsilon(\mathbf{R})=\epsilon_u(\mathbf{R})-\epsilon_g(\mathbf{R}). \quad (3.17)$$

$\Delta\epsilon$ is approximately equal to the energy the trapped electron acquires when it is excited from one state to another (the nuclear coordinates remain at $\mathbf{R}$). Actually, the difference in energy is related to all the electrons rather than just one.

Since we are interested in the q's, $\epsilon_u(\mathbf{R})$ is expressed as

$$\epsilon_u(\mathbf{R})=\epsilon_g(\mathbf{R})+\Delta\epsilon(\mathbf{R})=\epsilon_g(\mathbf{R}_g)+\tfrac{1}{2}\textstyle\sum_j\omega_j^2(g)q_j^2$$
$$+\Delta\epsilon(\mathbf{R}_g)+\textstyle\sum_j\epsilon_jq_j+\tfrac{1}{2}\sum_{jk}\epsilon_{jk}q_jq_k+\cdots, \quad (3.18)$$

where

$$\epsilon_j=[\partial\Delta\epsilon/\partial q_j]_{\mathbf{R}_g} \quad (3.18a)$$

and

$$\epsilon_{jk}=[\partial^2\Delta\epsilon/\partial q_j\partial q_k]_{\mathbf{R}_g}. \quad (3.18b)$$

The dimension of ϵ_j is (mass)$^{\frac{1}{2}}$ (length) (time)$^{-2}$ while the dimension of ϵ_{jk} is simply (time)$^{-2}$. The second term in (3.18) arises because $\epsilon_g(\mathbf{R})-\epsilon_g(\mathbf{R}_g)=\frac{1}{2}\sum_j\omega_j^2(g)q_j^2$, which follows from the definition of the q's.

At this point the theory runs into some difficulties. Equation (3.4) assumes that terms in $\Delta X_\alpha(j)\Delta X_\beta(k)\times\Delta X_\gamma(l)$ are so small that they can be neglected. If the q's are determined by thermal vibrations, they will be small at low temperatures. Equation (3.18) includes, however, the displacement which occurs during a transition, i.e., the difference between $\mathbf{R}_u$ and $\mathbf{R}_g$ defined by

$$[\partial\epsilon_g/\partial R]_{\mathbf{R}_g}=0 \quad (3.19a)$$

and

$$[\partial\epsilon_u/\partial R]_{\mathbf{R}_u}=0. \quad (3.19b)$$

Actual calculations of the difference between the $\mathbf{R}$'s have been made on some simple models. $\mathbf{R}_g-\mathbf{R}_u$ is about 0.3 A for the nearest neighbor in the case of a Tl^+ trap in KCl (W2) and 0.06 A for the self-trapped electron (M6). These results are to be compared to the root-mean-square displacement of an atom (Einsteinian model with a mass equal to 30 times that of the proton and frequency of 5×10^{12}). For $n=0$ (the quantum vibrational number), it is 0.06 A and increases to 0.13 A for $n=2$. X-ray measurements of the root-mean-square amplitude of vibration in NaCl at 86°K gives 0.15 A for Na^+ and 0.13 A for Cl^- (L3, p. 50). These large values must be attributed to the lower-frequency modes. The self-trapping calculations showed that the first anharmonic term was of no importance, due to a fortuitous geometry. However, this is not a general conclusion. If we include additional terms in (3.18), there seems to be no apparent simple way to relate the normal modes in the upper and lower states. Therefore, we consider (3.18) to be exact. For shallow traps and for any trap in nonionic crystals, this assumption must be *good*. It must also be a *fair* approximation for deeper traps in ionic crystals, such as the F center.

It is further assumed that the modes are nondegenerate. To those familiar with Fröhlich's phenomenological treatment, this may seem like a radical assumption indeed. One must remember that Fröhlich's approximation is not supported by detailed calculations

(M3). Secondly, we may be dealing to a large extent with local modes. This is supported by the analyses on the shape of the absorption bands. These are in the forbidden gap and cluster about a single value. There is no reason, however, to assume that the local modes are actually degenerate, and the above assumption is a natural one at the present stage of development. This assumption probably does not affect any major conclusions of this paper.

Now the transformation

$$q_j = q_j' + \sum_k{}' \frac{\epsilon_{jk}}{\omega_k^2(g) - \omega_j^2(g)} q_k' \tag{3.20}$$

is made. The prime on the sum indicates that $j \neq k$. Neglecting terms of order $\epsilon_{ij}\epsilon_{kl}$ or $\epsilon_j\epsilon_{kl}$ for $(k \neq l)$, (3.20) gives an orthogonal transformation. To the same approximation we write

$$\epsilon_u(\mathbf{R}) = \epsilon_g(\mathbf{R}_g) + \Delta\epsilon(\mathbf{R}_g) + \tfrac{1}{2} \sum_j \omega_j^2(u)(q_j')^2 + \sum_j \epsilon_j q_j' \tag{3.21}$$

$$\omega_j^2(u) = \omega_j^2(g) + \epsilon_{jj}. \tag{3.21a}$$

The new equilibrium position is obtained from (3.19b). Since the ΔX's are linear functions of the q's, (3.19b) gives

$$(\partial/\partial q_j')\epsilon_u = \omega_j^2(u) q_j' + \epsilon_j = 0. \tag{3.22}$$

The shift in the equilibrium position is

$$q_j' = -\epsilon_j/\omega_j^2(u). \tag{3.23}$$

Thus, the final transformation

$$Q_j = q_j' + \epsilon_j/\omega_j^2(u) = q_j' - \Delta q_j \tag{3.24}$$

gives the energy of the ground state in the form

$$\begin{aligned}\epsilon_u(\mathbf{R}) &= \epsilon_g(\mathbf{R}_g) + \Delta\epsilon(\mathbf{R}_g) - \tfrac{1}{2} \sum_j \epsilon_j^2/\omega_j^2(u) + \tfrac{1}{2} \sum_j \omega_j^2(u) Q_j^2 &(3.25)\\ &= \epsilon_u(\mathbf{R}_u) + \tfrac{1}{2} \sum_j \omega_j^2(u) Q_j^2. &(3.25\text{a})\end{aligned}$$

By direct substitution one may show that

$$\sum_j \left(\frac{\partial}{\partial q_j}\right)^2 = \sum_j \left(\frac{\partial}{\partial q_j'}\right)^2 = \sum_j \left(\frac{\partial}{\partial Q_j}\right)^2, \tag{3.26}$$

hence, the transformation does not modify T.

The first three terms on the right of (3.25) appear in the eigenvalue of h_e. The derivation serves to show the relation between the q's and Q's. This is of essential importance and not the final form of ϵ_u.

This concludes the formal treatment. The assumptions which have been made are now summarized to emphasize their limitations. These are that

(1) all cubic terms can be neglected;
(2) terms in $\epsilon_{ij}\epsilon_{kl}$ and $\epsilon_j\epsilon_{kl}$ for $k \neq l$ can be neglected; (3.27)
(3) the normal modes are nondegenerate.

In view of the work of Montroll and co-workers, we know that lattice perturbation can localize some of the modes. This effect does not appear above. The transformation (3.20) without the neglect of higher-order terms (item 2) may cause a radical change in the modes. This change most probably does not occur however during an electronic transition.

The third assumption probably is not a fundamental one, although the first two may be. The problem of degenerate modes is that the q's and p's of Eq. (3.6) are not unique. Consider two degenerate modes q_1 and q_2. The substitution $q_1'' = q_1 + q_2$ and $q_2'' = q_1 - q_2$ will not change the required form of the Hamiltonian, and the q'' modes are equally satisfactory. The additional terms which occur in the upper state put a requirement on the possible linear combination of the q's. These can be obtained from argument similar to those used in degenerate quantum mechanical perturbation theory. If we use the proper definition of the q's, the degenerate problem is similar to the nondegenerate one. For this reason, the author feels that item 3 is not an essential restriction. The author has not carried through the details of this argument. Certainly the transformations (3.20) and (3.24) allow one to make a simple synthesis of many theoretical ideas at a time when it is most needed from the experimental point of view. Hence, we assume their validity without any further ado.

For a point imperfection we may expect two types of ϵ_j. The ϵ_j's for the local modes will be especially large in solids with some polar characteristics. This leads to the LM approximation. The ϵ_j's for individual longitudinal modes are very small; the net effect, however, may be large. This leads to Hamiltonians similar to those employed by Fröhlich. For these modes the ϵ_{jj}'s must be extremely small and the transformation (3.20) need not be used.

Item 1 of Sec. 2 enters into the problem through (3.19b) or (3.24), item 2 through $\omega_j(g)$ or (3.21a), while item 3 arises through (3.12b) or (3.13b) depending on the form of Ψ employed.

The technique used on the F center by Huang and Rhys and by Pekar assumes that ϵ_j is of the order of $1/N$. This does not hold for local modes, hence the expansion techniques are questionable. O'Rourke does not require that $\epsilon_j \rightarrow 0$, in the first part of his paper, thus includes localized modes.

The division made above regarding the types of modes is not completely satisfactory since the Fröhlich description is somewhat oversimplified. The usual classification of modes, i.e., acoustical *versus* optical, transverse *versus* longitudinal, apply only to the long modes in polar crystals (M3). The majority of the modes actually have a wavelength of the order of several interionic distances and do not fit into the above classification. The experimentalist should remember that the LST relation is not completely reliable, and, therefore, should not take it too seriously. The theorist should attempt to formulate his equations in such a manner that he does not rely on the extreme simplification involved in this relation. As our understanding of the problems treated here increases (this involves further experimental data), we shall undoubtedly obtain much more reliable information regarding the vibrational modes in solids.

4. PHYSICAL INTERPRETATION OF OPTICAL AND THERMAL TRANSFORMATIONS

A physical interpretation of Sec. 3 is now attempted. It starts with a one-dimensional Franck-Condon diagram which will subsequently be elaborated. Next, the various activation energies are defined and their interrelations discussed. The results are applied to the V_1 center.

We start by considering the following simple model: The temperature is 0°K. Only one mode is affected by the transition. This implies that only one ϵ_j is different from zero. In Fig. 2 we plot ϵ_u and ϵ_g as a function of a coordinate q_j. It is convenient, for now, to set $\epsilon_{jj}=0$; hence $\omega_j(u)=\omega_j(g)$. Although ϵ is an eigenfunction of h_e, it is useful to divide it into two parts, namely, $\epsilon_g(\mathbf{R}_g)=\epsilon_g(0)$, which is considered as an electronic energy of the ground state, and $\epsilon_g(q_j)-\epsilon_g(0)$, which is considered as a lattice potential energy. This division is justified by Eqs. (3.14a and b). According to the simplified Franck-Condon principle, the system may absorb a photon and jump from point *a* to point *b* on ϵ_u. The use of the Born-Oppenheimer technique assumes that the electron has sufficient kinetic energy to occupy all the space required by $|\varphi'|^2$ before there has been an appreciable displacement of q_j from 0. ϵ_g has been replaced by ϵ_u, giving an additional "force" $-\epsilon_j$ on q_j. In the case considered in Fig. 2 $\epsilon_j=-\omega_j^2\Delta q_j$. Hence the total potential energy of the lattice relative to point *b* is $\frac{1}{2}\omega_j^2q_j^2+\epsilon_jq_j$ and its minimum appears at $q_j=-\epsilon_j/\omega_j^2$ in agreement with (3.23). As soon as the force on the q_j'th mode has changed, its equilibrium value has as well, although the ions are not at $-\epsilon_j/\omega_j^2$.

During the shift from *b* to *c*, $\Delta\epsilon$ *decreases* by $-\epsilon_j\Delta q=(\epsilon_j^2/\omega_j^2)$, while the potential energy of the lattice *increases* by $\frac{1}{2}\epsilon_j^2/\omega_j^2$, thus giving a total decrease of $\frac{1}{2}\epsilon_j^2/\omega_j^2$. Hence the third term of (3.25) is composed of two effects, the decrease of electronic energy and the increase of lattice energy. The simplicity of the interpretation arises because of the assumption that the restoring forces are not affected by the jump of the electron in the trap.

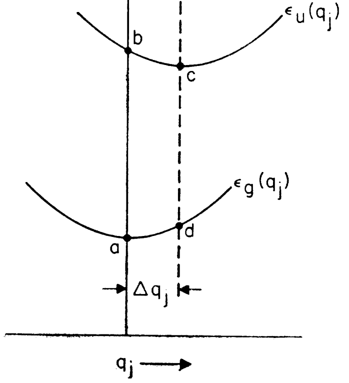

FIG. 2. Plots of ϵ_g and ϵ_u against q_j.

Quantum mechanics (still assuming that $\epsilon_{jj}=0$) only slightly modifies the picture. The stationary states are represented by horizontal lines since normal vibrations have kinetic as well as potential energy. The most probable transitions arise when the classical turning points of the upper and lower states occur for the same value of q_j. While this is the most probable, it is not the only one; indeed, the probability of "nonvertical" transitions explains the shape of the emission and absorption bands in solids.

The theory developed in Sec. 3 is now used to define the various types of activation energies. Neglecting the broadening due to the emission or absorption of phonons, the zero-point energy, and limiting our consideration to 0°K, we may define the following: activation energy for emission of a photon—E^e—$(c-d)$; activation energy for absorption of a photon—E^a—$(a-b)$; thermal activation energy which is the same for emission and absorption—E^t—$(a-c)$. The *a*, *b*, *c*, and *d* refer to Fig. 2.

As has been stressed previously, the Stokes' shift, which is the difference between E^e and E^a, is related to the third term of (3.25). After an absorption (from *a* to *b*), the force $-\epsilon_j$ is added, and the system relaxes by going to *c*. For $\epsilon_{jj}=0$, the stored energy after an emission equals the stored energy after an absorption, i.e.,

$$\epsilon_g(-\epsilon_j/\omega_j^2)-\epsilon_g(0)=\epsilon_u(0)-\epsilon_u(-\epsilon_j/\omega_j^2). \tag{4.1}$$

In (4.1) the arguments of ϵ_u refer to values of q not Q. Summarizing, the absorption activation energy includes the readjustment energies in both the upper and ground states; the emission activation energy excludes both, while the thermal includes the readjustment energy in only one state.

Although (4.1) was derived by considering the displacement of only one mode, it is quite general because ϵ_g and ϵ_u are functions only of the q's and not of the path taken. The displacements can be compared one by one to show that for an actual trap the total stored energy is the same in both states. In general then, one may write

$$E^e+2\delta E=E^t+\delta E=E^a \tag{4.2}$$

where δE is the readjustment energy $(\frac{1}{2})\sum_j\epsilon_j^2/\omega_j^2$, or

$$E^t=E^a-(1/2)(E^a-E^e)=(1/2)(E^a+E^e). \tag{4.2a}$$

If $E^e=0$, $E^t=\frac{1}{2}E^a$; hence, in general

$$E^t\geqslant(1/2)E^a \quad (\text{for } \epsilon_{jj}=0). \tag{4.2b}$$

In some problems we may be able to introduce an

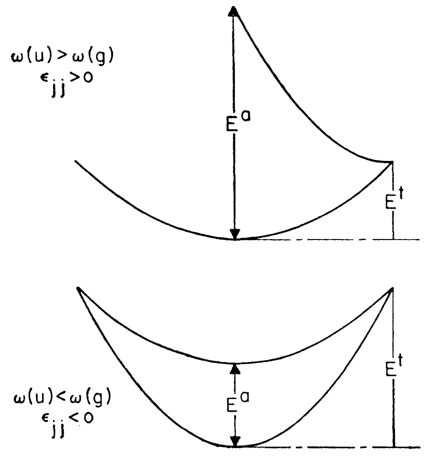

FIG. 3. Effects of ϵ_{jj} on E^a and E^t.

effective frequency (Secs. 9 and 10). In this case

$$\delta E=\tfrac{1}{2}\sum_j \epsilon_j^2/\omega_j^2=\hbar\omega\{\tfrac{1}{2}\sum_j \epsilon_j^2/\hbar\omega_j^3\}=\hbar\omega S \tag{4.3}$$

where ω is the effective frequency, defined by (4.3), and

$$S=\tfrac{1}{2}\sum_j \epsilon_j^2/\hbar\omega_j^3, \tag{4.3a}$$

the Huang-Rys factor. One may measure S directly for some transitions (Sec. 11). It is the ratio of the stored energy at b to the average effective phonon energy. For the F center in KCl, $S\approx 30$ (K4).

A relaxation of (4.2) occurs when $\epsilon_{jj}\neq 0$. When $\epsilon_{jk}(j\neq k)$ is small compared to ϵ_{jj}, the effect of the second derivative is to shift the frequencies of the modes. One may speak of a frequency shift superimposed on a displacement of the equilibrium position. Now (4.2b) does not apply, and E^t can be much smaller than $\frac{1}{2}E^a$. In other cases it can be even larger than E^a, as illustrated in Fig. 3,§ where only one mode is considered. If $E^t \ll E^a$, ϵ_{jj} must be of the order of ω_j^2. For $\epsilon_{jj}<0$, one obtains the strange case where $E^a<E^t$. However, the author knows of no such case in nature.

In the self-trapping calculations made by Seitz and the author (M6) for NaCl, items 2 and 3 of Sec. 2 were not considered; hence, $E^t=\frac{1}{2}E^a$. This gives 0.34 ev for E^t, not the value originally reported. The error arises from an erroneous formulation of Feynman's theorem (Eq. 3.16). The agreement between the calculation of Fröhlich, Pelzer, and Zienau (F3) and the reported value of E^t (i.e., 0.13 ev) must be fortuitous. The author believes that higher-order terms than ϵ_j must be included. Further, the mobility of the trap has to be included; hence the value 0.34 ev is a very preliminary one.

In view of the values of E^t and E^a for the F' center, the ϵ_{jj}'s must almost equal ω^2's for the local modes which cluster about negative-ion vacancies. The upper F' state corresponds to an F center and an electron in the conduction band. The lower state corresponds to two electrons in a negative-ion vacancy. To the approximation of interest here we may assume that the free electron does not interact with the modes. $\Delta\epsilon(\mathbf{R})$ of Eq. (3.17) is simply the binding energy of the second electron in the F' center. Since there is a radical difference in the upper and lower states, the assumption of $\epsilon_{jj}\approx\omega_j^2(g)$ seems plausible. The author finds it hard to believe that a corresponding situation exists for a hole trapped at a positive-ion vacancy. One assumes that it possesses two bound states. This is Seitz's model for the V_1 band in KCl and KBr. The hole must be spread out similar to an electron in the F center. Transitions of the hole from an excited to a ground state could influence the vibrational frequencies but hardly enough to change the activation energy from 3.0 ev to 0.23 ev. Our present knowledge of the V centers is so meager that the possibility of an alternate interpretation of the experiment should not be overlooked.

5. PROPERTIES OF THE TOTAL HAMILTONIAN

In Sec. 3 a theory was developed which is completely general, provided one may use the Born-Oppenheimer technique. In this section we compare this development to alternate formulations of the problem in order to contrast the ideas. We also compare the development of Sec. 3 with some problems in electrodynamics, in particular, to contrast the behavior of phonons and photons.

In complex systems one likes to split the Hamiltonian into parts which interact only slightly. Thus, in electrodynamics, it is divided into the radiation field H_{rad}, the part related to the charged particles H_{el}, and the interaction term H_{int}, which relates the electrons to the photons. One usually develops expressions for H_{rad} and H_{el} without regard to each other. The introduction of an electron in a vacuum does not affect H_{rad}, nor does the introduction of black-body radiation affect H_{el}. When one considers a trapped electron in an electromagnetic field one adds H_{int} to $H_{\text{rad}}+H_{\text{el}}$ without modifying either.

The solid state problem is more complex, and the method of splitting the Hamiltonian depends on the problem at hand. Once Ψ is selected, the term corresponding to H_{int} is given by (3.12b) or (3.13b). The problem is to split $H_0(A)$ or $H_0(S)$ in two. These we denote by H_e and H_L. In general, H_e and H_L are intimately coupled and cannot be separated. One may use a purely mathematical argument like Born and Oppenheimer (B, p. 166) to evaluate the importance of the various terms. The convergence of the approximation has not been studied, however. Crude calculations show that the adiabatic approximation must be used with caution for shallow traps (M4). The splitting procedure is discussed in a semi-intuitive manner; further analytical proofs are most desirable.

---

§ In Fig. 3, the problem of the intersection of the potential curves has not been considered.

(a) Trapped Electron

For an electron trapped at a point imperfection, we may use (3.1) or a form which is related more closely to the way actual calculations are made. For the latter purpose we define the impurity center Hamiltonian. With proper care one may make the treatment completely rigorous. Thus we write

$$H = t + T + V_L(\mathbf{R}) + V_I(\mathbf{R}) + V_e(\mathbf{R},\mathbf{r}). \qquad (5.1)$$

Here t is the kinetic energy of the trapped electron; $V_L + V_I$ is the interionic or interatomic potential; $V_e(\mathbf{R},\mathbf{r})$ is the potential energy due to an excess electron at $\mathbf{r}$ when the ions (or atoms) are at $\mathbf{R}$.

It is convenient for pedagogical purposes to split $V_L + V_I$ into two parts. V_L is the potential energy for the perfect lattice, and V_I arises from the point imperfection. Thus, in the case of the F center, V_I is due to the negative-ion vacancy. Mott and Littleton considered this problem (M12), so one may call V_I the Mott-Littleton term. In the more conventional treatment, $V_L + V_I$ arises from the coulombic and repulsive forces of the crystal. In treatments using the Born-Oppenheimer technique, it arises from the eigenvalue of an electronic Hamiltonian which includes all the electrons except the trapped one (B, p. 173).

First, deep traps are considered; hence, we are required to use the adiabatic approximation. Equation (3.13) gives

$$\begin{aligned}(H_L + H_e)\varphi(\mathbf{R})\chi &= H_0(A)\varphi(\mathbf{R})\chi \\ &= \varphi T\chi + (t + V_L + V_I + V_e)\varphi\chi, \qquad (5.2)\end{aligned}$$

$$H_1(A) = H - H_0(A). \qquad (5.2\text{a})$$

There is a striking contrast between our problem and a photon field. The splitting in electrodynamics is done purely classically and in an elegant manner. Here we have had to introduce quantum mechanical operators and further assume an approximate wave function. How does one split H_0 into two parts?

Following the development in Sec. 3, we expand about $\mathbf{R}_n$ defined by

$$\left\{\frac{\partial}{\partial X_\alpha(k)}[\Delta\epsilon_n + V_L + V_I]\right\}_{\mathbf{R}_n} = 0. \qquad (5.3)$$

$\Delta\epsilon_n$ is an eigenvalue of $t + V_e(\mathbf{R},\mathbf{r})$. We split $H_0(A)$ by writing

$$H_L = T' + V_L + V_I + \Delta\epsilon_n(\mathbf{R}) - \Delta\epsilon_n(\mathbf{R}_n) \qquad (5.4)$$

and

$$H_e = t + V_e. \qquad (5.5)$$

T' means that T only operates on χ. We note that

$$H_0 \neq H_L + H_e. \qquad (5.6)$$

When the sum operates on $\varphi\chi$ an extra function $\Delta\epsilon_n(\mathbf{R}) - \Delta\epsilon_n(\mathbf{R}_n)$ appears. H_L includes approximately the cohesive energy of the distorted crystal.‖

The modes defined by (5.3) and (5.4) depend on the state of the electron due to the presence of $\Delta\epsilon_n$. Using the foregoing development, we may understand the various simplifications that have been made.

(1) The phenomenological approach (a) ignores the presence of V_I and (b) makes a crude approximation of the actual Hamiltonian by assuming that the equation

$$\{H_L - V_I - \Delta\epsilon_n(\mathbf{R}) + \Delta\epsilon_n(\mathbf{R}_n)\}\chi = \epsilon_v\chi \qquad (5.7)$$

gives pure longitudinal and pure transverse optical modes. It further assumes that the lower branches are pure acoustical.

These extreme simplifications are inadequate for some problems involving normal modes in alkali halides. The interaction between the trapped electron and the phonons is obtained by adding $\Delta\epsilon_n$ to (5.7); namely, one requires solutions of the following equation:

$$\{H_L - V_I\}\chi = \epsilon_v\chi. \qquad (5.8)$$

In principle the inclusion of $\Delta\epsilon_n$ leads to no difficulties, and the method developed in Sec. 3 can be employed. Meyer has developed a perturbation scheme using V_e. This, however, leads to the omission of some terms. In Appendix II we compare both methods.

(2) The local modes approach: One assumes that the eigenequation

$$H_L\chi = \epsilon_v\chi \qquad (5.9)$$

gives two types of modes, q_i, which are local, and q_c, which pertain to the perfect crystal. For this approach to be valid, $\Delta\epsilon_n$ must be independent of the q_c. If $\Delta\epsilon_n$ is only a function of a single localized mode then we have the CC model. The $\Delta\epsilon$'s can again be used to calculate the effect of the trapped electron on the modes. *A priori*, there is no clear reason for believing that $\Delta\epsilon_n$ will be independent of the q_c's. Hence, there is no apparent reason to assume that $\Delta\epsilon_n$ will not be a function of the q_c's. Only extremely complex calculations, not available at present, could tell the exact form of $\Delta\epsilon(q_i,q_c)$. One may resolve this problem somewhat by obtaining equations for the shape of absorption and emission bands in solids with adjustable parameters. These parameters can be evaluated by analysis of the experimental data. This, in turn, will give basic information regarding the relations among $\Delta\epsilon_n$, q_c, and q_i. Part II of this paper is devoted to this problem.

(b) Free Electron

Consider next a free electron in a metal or semiconductor. Two arguments suggest that the Born-Oppenheimer technique should not be used. First, consider the effect a free electron at $\mathbf{r}$ has on the modes. Its behavior is described by means of a wave packet

---

‖ Approximately because we use $\mathbf{R}_n$ defined by Eq. (5.3) instead of the values of $\mathbf{R}$ determined by minimizing V_L or $V_L + V_I$.

made from Bloch functions. The electron proceeds in a straight line for about 200 A and then gets reflected through an angle. If the electron has the energy of 3 ev (approximately the Fermi level of a metal) it collides with the lattice every 2×10^{-14} sec. It is not confined to a local region, but wanders in random fashion, so that an average effect over a period of vibration is meaningless. Analytically, for a pure Bloch function, ϵ_j equals zero, so such an electron does not exert a force on the normal modes as shown below. Therefore, one splits the system's Hamiltonian as follows ($V_I=0$)

$$H_L=T+V_L(\mathbf{R}) \tag{5.10a}$$

$$H_e=t+V_e(\mathbf{R}_L) \tag{5.10b}$$

and

$$H_1=V_e(\mathbf{R})-V_e(\mathbf{R}_L) \tag{5.10c}$$

to obtain the usual theory (W4-Chap. IX). The normal modes about $\mathbf{R}_L$ are determined from V_L. Here another assumption is made, that one should use $\varphi(\mathbf{R}_L)$ rather than $\varphi(\mathbf{R})$. The continuously readjusting wave function requires a type of kinetic energy, and one suspects that the loss in potential energy does not compensate for this gain (M4).

The distinction between the static and the adiabatic approximation is academic, since, as Haug (H2) has shown, that first-order perturbation theory gives the same results for both. The treatment assumes that one does not use the Born-Oppenheimer technique for the free electron—that is, that H_L determines the q's. This requires that $\epsilon_j(\mathbf{R}_L)=0$. Proof of this relation for a Bloch electron is now given.

The interaction between an electron and the lattice in the conduction band has the form

$$H_1=\sum_j a_j\Lambda_j, \tag{5.11}$$

where the Λ_j's are determined from (5.10a). To a sufficient approximation we write

$$a_j=\text{const}\exp(i\mathbf{k}_j\cdot\mathbf{r}) \tag{5.12}$$

where $\mathbf{k}_j$ is the wave-number vector of the jth mode. The Bloch function for a conduction electron may be written in the form

$$\varphi_p=u_p(\mathbf{r})\exp(i\mathbf{p}\cdot\mathbf{r}) \tag{5.13}$$

where $\mathbf{p}$ is the momentum vector and u_p has the periodicity of the lattice. Hence from (3.16) it follows that

$$\epsilon_j=\langle\varphi_p|a_j|\varphi_p\rangle=\text{const}\int u_p^2\exp(i\mathbf{k}_j\cdot\mathbf{r})d\tau=0 \tag{5.14}$$

since u_p is periodic. This shows that the Λ_j's describe the true modes.¶ This argument also applies to nonpolar semiconductors.

This proof as it stands should apply to polar crystals as well. Detailed considerations show that this development is incomplete. This follows because some ϵ_{jj} are zero in spite of the fact that $\Delta\epsilon_n(\mathbf{R})$ is not small. For this case H_1 has a major influence on the q's, and the presence of the electron may generate a new set of modes. Here the problem does not correspond to the one in electrodynamics.

Applying this approach, Eq. (5.10), to deep traps where the electron's kinetic energy is large, (5.14) does not hold, and exceptionally large values of the interaction are obtained, simply because the q's derived from (5.10) are not the appropriate ones. These χ's form an orthogonal set, although a force $-\epsilon_j(\mathbf{R}_L)$ remains on the nuclei at $\Lambda_j=0$.

(c) Comparison with Quantum Electrodynamics

Coming now to some general comparisons between quantum electrodynamics and the theory developed here, no equation in quantum electrodynamics corresponds to (3.4a). First, consider case b where all the $\epsilon_j(\mathbf{R}_L)$'s are zero and the Λ's are the true modes. Hence H_{rad} corresponds to H_L, H_{el} corresponds to H_e, and H_{int} corresponds to H_1. The frequency and wavelength of the photon modes are determined for free space and are not influenced by the electrons, although their number is determined in part by electronic transitions. The number of phonons is also determined by the electronic state, if we use time dependent perturbation theory, although the q's are obtained from H_L. The polaron problem in semiconductors and metals corresponds to the self-energy problem in electrodynamics. This is also true for many optical problems in valence semiconductors, i.e., such as the band-to-band transition in germanium, silicon, and diamond. Here the normal modes do indeed behave in a manner similar to photons, and the word "phonons" is most appropriate.

This is to be contrasted to the situation where method (a) should be used. The term which mixes the electronic and normal mode wave functions or causes transition is $H_1(A)$ of (5.2a). The ϵ_j's and ϵ_{jj}'s have no counterpart in quantum electrodynamics. They generate a new set of q's for every electron level and cause an essential difference between the two fields. Their presence makes multiphonon processes natural in some solids. In this case, optical problems are similar to those occurring in diatomic molecules (Part II). The similarity between phonons and photons breaks down. If one applies method (b) to polar crystals, there is no simple way to separate the energy associated with the poor choice of the modes and that caused by $H_1(S)$.

Thus we have two types of problems in phonondynamics. In one the ϵ's can be ignored and use can be made of the tools of modern electrodynamics. In the other, we are in a different domain, where the ele-

---

¶ One may arrive at the expression for ϵ_j in a more rigorous manner. In general $\langle\varphi_q|H_1|\varphi_p\rangle\neq0$ only if $\mathbf{p}-\mathbf{q}\pm\mathbf{k}=0$ [W4, Eq. (9.3.3) with $\mathbf{g}_b=0$]. Here $\mathbf{p}=\mathbf{q}$; hence, for $\mathbf{k}_j\neq0$, $\epsilon_j=0$.

mentary concepts of electrodynamics do not serve as a guide. The first situation is in a sense a "special" case.

6. CONCLUSIONS OF PART I

1. By the use of the Born-Oppenheimer method, we have shown what effects electron transitions have on the normal modes of vibration. The problem has been formulated in a new manner to show the interrelation of the various terms. The two major effects are (a) a shift in the equilibrium position of the normal modes—first-order effect; (b) a change in the frequencies of vibration—second-order effect. The analytical reason for these shifts is shown and related to the change in the electronic binding energies of traps. The relations which are derived from the microscopic Hamiltonian are completely general. It was indicated why one would not expect the calculations made by Huang and Rhys, by Pekar, and by Lax to apply to an F center. To obtain an accurate theoretical expression, greater care must be taken in the use of various expansions.

2. Various activation energies are defined and general relations obtained between them. These impose restrictions on the interpretation of some experiments done on color centers.

3. A comparison has been made of quantum electrodynamics and phonondynamics. Terms not present in the former arise. They account for multiphonon processes. These additional terms play a very important role in the shape of optical absorption and emission bands. They may enter into the polaron problem. The electron in the conduction band of some polar solids may create new local modes about itself. These local modes do not appear in electrodynamics, hence the polaron problem in some crystals is not equivalent to problems in electrodynamics. These terms make it possible for a hole to be self-trapped, as indicated by the experiments of Castner and Kanzig (C1). To understand the stability of some of the new types of centers, the molecular color centers, we must examine the phonon-electron Hamiltonian discussed here in fuller detail.

Part II. Broadening of Absorption Lines Due to Multiphonon Processes

7. INTRODUCTION TO PART II

In the following sections the theory developed in Part I is applied to the broadening of absorption bands in solids. We only consider transitions between two bound states. The breadth of a line may be due to several causes.

(a) One is the Heisenberg principle which requires an uncertainty in the energy of a level, provided its lifetime is finite. An alternate way of looking at this problem is to use higher-order terms in the standard time-dependent perturbation theory (H3, p. 181). This explains the breadth of the hydrogenic lines at low pressure. The breadth of lines due to this effect should be very roughly of the order of that observed in atoms.

TABLE II. Breadth of absorption lines in ev.

Atomic	
One of the H_α lines of hydrogen	3×10^{-6}
A very wide atomic line of CuI ($^4F_{\frac{5}{2}}-{}^4D_{\frac{3}{2}}$ at 4540 A)	6×10^{-4}
Solids	
The 278 cm^{-1} line of B doped Si	7×10^{-4}
The F center breadth in KCl at 0°K	0.16
The F' center breadth in KCl	about 1
A narrow band in LiF (P5)	0.01
Energy of one optical phonon	0.01–0.08

(b) Broadening is also caused by the interaction between centers. We must assume that there is more than one trap in a solid so that (5.1), which applies only to an individual imperfection, does not contain the whole Hamiltonian. Their sum does not form the total Hamiltonian, for one must consider interactions between centers. Without these additional terms, ϵ_u represents a highly degenerate level, since any imperfection can be excited. With the interaction terms, the degeneracy of ϵ_u is removed, and the excited states spread out into a narrow band. Since no detailed calculation has been made, it is not known whether the degeneracy of ϵ_u can be completely removed. If a crystal has 5×10^{16} centers per cc, the mean separation is 270 A. This type of interaction must be small in polar solids, since 270 A is large compared to the spread of the electron wave functions. For example, the excited state of the F center in KCl does not extend beyond 13 A (Smith, S6). The interaction may not be small if the imperfection is such that the spread in the wave function is of the order of the distance between centers.

(c) Although this effect may make a small contribution to the broadening of an absorption line in solids, our interest is in the fact that during an optical transition no strict selection rules apply to the v_j's. If $\epsilon_j=\epsilon_{jj}=0$, strict rules would apply, and this effect would not make a contribution to the problem.

Effects (a) and (b) are essentially temperature independent, while (c) depends strongly on the temperature.

In view of the complexity of the problem, equations are derived with parameters which are to be evaluated experimentally. This is the first necessary step, since at present our knowledge is far too meager to attempt exact *a priori* calculations. Some experimental facts will be presented before embarking on the theoretical details.

The width of lines varies over a large range. Some typical values are given in Table II. Thus the width of some lines in solids approaches the broadest found in atomic spectra. In general, lines in solids are considered broader, however. In polar crystals some bands are very much wider, and the absorption or emission of a single phonon will not explain the phenomenon. The marked temperature dependence of the shape of some lines strongly suggests that (c) can dominate the others. Detailed studies (M5, K4) support this conclusion.

The theory developed here does not apply to the F' band since the upper state is not bound. It is not completely clear why some bands in polar materials are extremely narrow. One may simply assume that certain parameters, to be derived, are very small. On the other hand, more complex concepts may be involved, such as the breakdown of the Born-Oppenheimer technique; further studies are required. The theory developed applies to bands whose width is approximately equal to the F center and is temperature dependent.

Experimentally, the absorption, α, is measured as a function of the wavelength or the photon energy ϵ (in ev). The observed $\alpha(\epsilon)$'s are not simple analytical curves; hence a way must be found to characterize them. We may in general define: ϵ_m, the value of ϵ where α has its maximum value, α_m; ϵ_r is where α has half its maximum value on the red side of ϵ_m, and ϵ_v is the corresponding point on the violet. Further useful definitions follow:

the moments— $$M_n=\int_0^\infty \alpha(\epsilon)\epsilon^n d\epsilon \tag{7.1}$$

the average— $$\bar{\epsilon}=M_1/M_0 \tag{7.2}$$

$$m^2=\frac{1}{M_0}\int_0^\infty (\epsilon-\bar{\epsilon})^2\alpha(\epsilon)d\epsilon \tag{7.3}$$

and the half-width— $$H=\epsilon_v-\epsilon_r. \tag{7.4}$$

In general,

$$m^2=(M_2/M_0)-\bar{\epsilon}^2. \tag{7.5}$$

The absorption is due to upward transitions induced by the vector potential of the light which falls on the crystal. To relate the measured absorption at photon energy ϵ to the transitions, four factors must be considered.

(1) The vector potential at the imperfection has to be related to the intensity of light falling on the crystal. Lorentz suggested a way of doing this. It is not known whether his theory applies rigorously to traps in solids and deviations from his simple equation would not be surprising. In any case the Poynting vector (the light intensity) is proportional to the square of the vector potential at the imperfection.

(2) The second factor is due to the φ's which give matrix elements. The expression may be simplified by the introduction of an oscillator strength, f. Classically, the second item contains no unknown since f equals unity. Quantum mechanically, the problem requires exact wave functions, which at present are unknown. Most probably, we shall have to introduce the f factor empirically for some time to come.

(3) The imperfection concentration.

(4) Finally, one must consider the shape factor. This can be done by multiplying the usual atomic absorption equation, item (2), by a function $G_n(\epsilon)$. G_n arises from items (a), (b), and (c) considered previously. In all cases studied so far, G_n has the property $\int G_n(\epsilon)d\epsilon=1$.

The measured absorption at ϵ is the product of the above four factors. If one could make exact calculations, the impurity concentration could be treated as an unknown and computed from a single point, ϵ. Even without an exact calculation, one might evaluate the factor associated with (1) and (2) from experimental data and obtain the concentration with the use of a single constant. This would require a detailed knowledge of G_n, which is lacking. The G_n can be eliminated by an integration over ϵ. This procedure is impractical in many cases, for one cannot measure the absorption at the wings of the band (due to overlapping from other absorption bands). The integration technique is also extremely lengthy. Many years ago Smakula suggested replacing $\int\alpha(\epsilon)d\epsilon$ by a product of α_m times H. This requires the introduction of a constant a_s such that $a_sG_mH=1$, where G_m is the peak value of G.

To illustrate this procedure, let us assume that G_n has the triangular shape, i.e.,

$$\begin{aligned} G_n&=0 && \text{for } \epsilon>a\\ &=(1/H)(a-\epsilon/a-\epsilon_m) && \text{for } a>\epsilon>\epsilon_m\\ &=(1/H)(\epsilon-b/\epsilon_m-b) && \text{for } \epsilon_m>\epsilon>b\\ &=0 && \text{for } b>\epsilon. \end{aligned} \tag{7.6}$$

The area under G_n is unity. The integration over the frequency equals G_mH and $a_s=1$ for the shape given by (7.6). Hence, the product G_mH or α_mH eliminates the fourth factor. The advantage of this procedure is that the temperature dependence of H seems to be eliminated.**

The essence of Smakula's famous equation is the substitution of G_mH for $\int G(\epsilon)d\epsilon$, not the exact form of $G_n(\epsilon)$. Therefore we refer to the general equation by his name and call a_s Smakula's constant. In this equation a_s is always multiplied by two factors arising from (1) and (2); hence the actual value of a_s is of little experimental importance. Nevertheless, a_s is a measure of the shape of an absorption band, as are the variables defined in Eq. (7.1) to (7.5).

It is useful to determine H, m, and a_s for several types of $G_n(\epsilon)$, namely,

The Gaussian

$$G_n=\frac{a}{\sqrt{\pi}}\exp\{-a^2(\epsilon-\epsilon_m)^2\}. \tag{7.7}$$

** "Seems to be," since there is practically no experimental data to support or refute this assumption.

Hence,

$$H(G)=\frac{1}{a}[4\ln 2]^{\frac{1}{2}}. \tag{7.7a}$$

Further

$$m^2=(1/2a^2)=(1/8\ln 2)H^2=(1/5.545)H^2 \tag{7.7b}$$

and

$$a_s(G)=(1/G_mH)=[\pi/4\ln 2]^{\frac{1}{2}}=1.0645. \tag{7.7c}$$

The Lorentzian

$$G_n=\frac{b}{\pi}\frac{1}{[1+b^2(\epsilon-\epsilon_m)^2]} \tag{7.8}$$

Now

$$H(L)=(2/b) \tag{7.9a}$$

and

$$a_s(L)=(\pi/2)=1.5708. \tag{7.9b}$$

M_2 does not exist for (7.8).

The Double Gaussian

G_n might be made of two Gaussians, one for the violet side with $a=a_v$ and another for the red side, with $a=a_r$. Then

$$G_m=(2/\sqrt{\pi})[(1/a_r)+(1/a_v)]^{-1}, \tag{7.10}$$

$$H(DG)=(\ln 2)^{\frac{1}{2}}[(1/a_r)+(1/a_v)], \tag{7.11a}$$

$$m^2=\tfrac{1}{2}[(1/a_r)+(1/a_v)]^{-1}\times[(1/a_r^3)+(1/a_v^3)], \tag{7.11b}$$

and

$$a_s(DG)=a_s(G)=1.0645. \tag{7.11c}$$

Various attempts have been made to describe the shape of the absorption band associated with F centers and all three types have been considered. One of the most successful is the double Gaussian. For this curve a_s is the same as for the single Gaussian.

The Pekarian

This curve is discussed in Sec. 9 and Appendix IV. To obtain $a_s(P)$, numerical integration techniques were used, since the analytic form is complex. It actually depends on H. However, unless the half-width is very small,

$$m^2=H^2/5.57 \tag{7.12a}$$

and

$$a_s(P)=1.07, \tag{7.12b}$$

which agrees with Eqs. (7.7b) and (7.7c). A Pekarian curve resembles a double Gaussian, so that the similarity of $a_s(P)$, $a_s(G)$, and $a_s(DG)$ is not surprising.

In Smakula's original derivation $a_s(L)$ was used. In recent years experimental studies indicate that the Gaussians or double Gaussians give better agreement with the observed curves. Dexter has suggested that one might replace $a_s(L)$ by $a_s(G)$. There are good arguments for this change. The absorption shapes, however, are not true Gaussians, and the suggestion simply means that we replace one empirical constant with another without gaining any fundamental information. There is some evidence that the band shape is Pekarian.

Since in Smakula's equation a_s is always multiplied by two other factors, the actual value of a_s is of little experimental importance. The danger in making the change is that confusion will result. The day may come when one will know the true form of G_n and have a correct expression for a_s. As this day has not yet arrived, the standard form of Smakula's equation is preferable.

8. GENERAL FORMULATION OF ABSORPTION PROBLEM

In this section the absorption problem is formulated in general. The next two sections discuss the shape and moments. Since deep traps are to be considered, the adiabatic approximation must be used. The electron-phonon interaction term, i.e., (3.13b), will be ignored. The Hamiltonians of the solid can therefore be written in the forms: for the ground state

$$H_g=\epsilon_g(\theta)+T_g'+V_g \tag{8.1}$$

or

$$E=\epsilon_g(\theta)+\textstyle\sum_j \hbar\omega_j(g)(v_j+\frac{1}{2}), \tag{8.1a}$$

while for the excited state

$$H_u=\epsilon_u(\theta)+T_u'+V_u \tag{8.2}$$

or

$$E'=\epsilon_u(\theta)+\textstyle\sum_j \hbar\omega_j(u)(v_j'+\frac{1}{2}), \tag{8.2a}$$

where v_j is the vibrational quantum number of the jth mode when the electron is in the ground state, while v_j' corresponds to the upper state; ϵ_g and ϵ_u are evaluated at $\mathbf{R}_g$ and $\mathbf{R}_u$, (3.19a) and (3.19b) $H_{g,u}$ is an operator, while E is the total energy, (3.14a). V_g and V_u are $\epsilon_g(\mathbf{R})-\epsilon_g(\mathbf{R}_g)$ and $\epsilon_u(\mathbf{R})-\epsilon_u(\mathbf{R}_u)$, respectively [see Eq. (3.4)].

Effects of thermal expansions are not included in the theory of Part I. The thermal expansion of the crystal arises from the dependence of the vibrational frequencies on the volume (Slater, S5, p. 199). In principle, the thermal expansion may influence all the variables. It is believed that the primary effect of the temperature (θ) is on ϵ_g and ϵ_u.

To arrive at an expression for the absorption coefficient, we start with the standard equation for the energy absorbed by an atom when light falls on it (2 of Sec. 7). This expression must be corrected for the presence of the medium and for various broadening effects, as discussed in the last section (1 and 4). Since Dirac's delta functions are used, special care must be employed. First-order perturbation theory gives the following expression for the energy absorbed by an atom in a

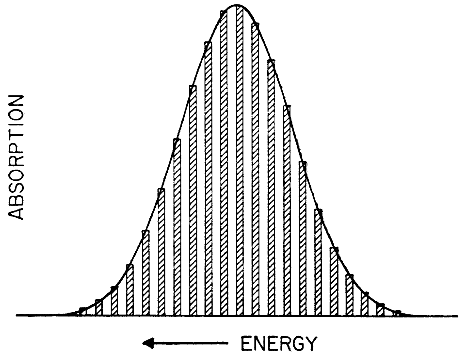

FIG. 4. Schematic diagram showing the broadening due to the emission or the absorption of phonons.

vacuum (H3, p. 180):

$$s_{\text{atom}}=\frac{4\pi^2}{3}\frac{e^2}{\hbar c}\nu|\{\langle\Psi'(A)|\mathbf{r}|\Psi(A)\rangle\}|^2 I_\nu, \qquad (8.3)$$

where ν is the angular frequency of the absorbed light[††]; $\Psi'(A)$ and $\Psi(A)$ are the total wave functions for the ground and excited states, Eq. (3.11); and I_ν is the intensity of the light per unit angular frequency interval, i.e., the energy of the light which falls on the crystals in the angular frequency interval $\Delta\nu$ is $I_\nu\Delta\nu$.

In a medium, the following modifications must be made.

(1a) If n_0 is the high-frequency dielectric constant, the intensity I_ν (Poynting vector) is $(cn_0F^2/4\pi)$. Since the transition is caused by F^2, (8.3) must be divided by n_0.[§§]

(1b) The space average field must be replaced by the local field. Since they are proportional to each other, we introduce a constant bn_0. For a Lorentz local field $b=(1/9n_0)(2+n_0^2)^2$ (B, p. 100).

(2) As discussed, lines have a finite width.

(1a) and (1b) correspond to 1 of Sec. 7. (2) corresponds to the broadening due to the uncertainty principle and the interaction between neighboring centers. If (8.3) is multiplied by b, the effects of (1a) and (1b) are included.

(2) requires the introduction of the function $g(\nu)$ with the following properties; it peaks at

$$\nu=[E'-E]/\hbar \qquad (8.4)$$

and

$$\int_0^\infty g(\nu)d\nu=1. \qquad (8.5)$$

The g does not include the effects of the ϵ_j's and ϵ_{jj}'s and is not the same as G_n. Figure 4 illustrates the problem. There is an over-all absorption band and a fine structure. We may expect to observe the fine structure only if the half-widths of the g's are less than the energy of one phonon (i.e., $\hbar\omega$). Figure 4 assumes that one is dealing with a single phonon frequency. When a center interacts with phonons of several frequencies, i.e., if there is dispersion, the ϵ_j's and ϵ_{jj}'s can cause a broadening of the "lines" shown in Fig. 4. This problem has been discussed by Krivoglaz and Pekar (K5). There seems to be no simple way to separate this effect from those discussed in Sec. 7. This effect is not considered further here.

We now digress slightly to indicate how the trap-trap interaction produces a broadening. The breadth of an electron-spin resonance line also arises from two effects: one is because of the interaction between the spins (spin-spin), and the other is because of the interaction of the electron with the magnetic moments of the surrounding nuclei (hyperfine). The hyperfine interaction often has a much larger effect. The problem is thus similar to the one considered here. Strangely enough, we have a much better understanding of the broadening problem in the newer field (electron-spin resonance).

For this development the solid is considered to be a large molecule of unit volume. There will therefore be N imperfections. We ignore the lattice vibrations, hence denote by $\mathbf{R}_j$ the rest position of the jth imperfection, and by $\mathbf{r}_j$ the position of its electron (relative to $\mathbf{R}_j$). Again two bound states per trap are assumed. The total ground state eigenfunction has the following form in the zeroth approximation, where the interactions between imperfections are ignored,

$$\Phi_0(g)=\Pi^j\varphi(\mathbf{R}_j+\mathbf{r}_j). \qquad (8.6)$$

(8.6) uses the Hartree approximation (S2, p. 234), while the excited state is of the form

$$\Phi_0(u_1k)=\varphi(\mathbf{R}_1+\mathbf{r}_1)\cdots\varphi(\mathbf{R}_{k-1}+\mathbf{r}_{k-1}) \times\varphi'(\mathbf{R}_k+\mathbf{r}_k)\varphi(\mathbf{R}_{k+1}+\mathbf{r}_{k+1})\cdots\varphi(\mathbf{R}_N+\mathbf{r}_N). \qquad (8.7)$$

It is N-fold degenerate, since any imperfection can be excited.

We next consider two perturbations: (1) due to the optical waves and (2) due to the imperfection-imperfection interaction. The first has the form [H3, Eq. (13.7)],

$$\textstyle\sum_j(e/mc)\mathbf{p}_j(e)\cdot\mathbf{A}(\mathbf{R}_j+\mathbf{r}_j), \qquad (8.8)$$

where $\mathbf{p}_j(e)$ is the electron's momentum and $\mathbf{A}$ is the vector potential. If one combines (8.6), (8.7), and (8.8) with the usual theory of absorption (H3, p. 143 and p. 179), the following transition matrix is obtained,

$$|\langle\Phi_0(u,k)|\mathbf{R}_{\text{eff}}|\Phi_0(g)\rangle|^2 \qquad (8.9)$$

where

$$\mathbf{R}_{\text{eff}}=\textstyle\sum_j\mathbf{r}_j\exp(-i\boldsymbol{\kappa}\cdot\mathbf{R}_j) \qquad (8.9a)$$

[††] The angular frequency of an electromagnetic wave is denoted by ν, while the angular frequency of a phonon is ω. The use of ν as an angular frequency is not the usual practice, but it has been used in one standard treatment (H3).

[§§] The permeability is assumed to be unity (A1, p. 188). F is the electric field strength.

and $\boldsymbol{\kappa}$ is the wave vector (ν/c) of the exciting light. The total effect is a sum of (8.9) over all the upper states. In this approximation (8.9) is just $N|\langle\varphi'|\mathbf{r}|\varphi\rangle|^2$, as one would expect.

The second perturbation produces changes in (8.6) and (8.7). We first apply the trap-trap interaction and then use (8.8). Since $\Phi_0(g)$ is nondegenerate, its energy level will be slightly shifted. The perturbation, however, will affect $\Phi_0(u,k)$ more profoundly. It removes some or all of the degeneracy and the upper level will fan out (Fig. 5). The various eigenfunctions are denoted by $\Phi_1(u,k)$. One may no longer replace $\mathbf{R}_{\mathrm{eff}}$ by $\mathbf{r}$, since the phase factor is of utmost importance; hence, the matrix element becomes

$$\langle\Phi_1(u,k)|\mathbf{R}_{\mathrm{eff}}|\Phi_1(g)\rangle. \tag{8.10}$$

Many of the cross terms in the square of the matrix cancel due to the random distribution of the $\mathbf{R}_{\mathrm{eff}}$. The old theory of spectroscopic stability (V1, p. 137) gives some useful information. It can be applied directly to (8.10) to show that

$$\sum_k^N|\langle\Phi_0(u,k)|\mathbf{R}_{\mathrm{eff}}|\Phi_0(g)\rangle|^2=N|\langle\varphi'|\mathbf{r}|\varphi\rangle|^2$$
$$=\sum_k^N|\langle\Phi_1(u,k)|\mathbf{R}_{\mathrm{eff}}|\Phi_1(g)\rangle|^2. \tag{8.11}$$

The perturbation is assumed to be small enough that the $\Phi_1(u,k)$'s can be expanded in terms of the $\Phi_0(u,k)$'s.

The next step is to define $g(\nu)$ by the relation

$$\sum_{\nu-\frac{1}{2}\Delta\nu}^{\nu+\frac{1}{2}\Delta\nu}|\langle\Phi_1(u,k)|\mathbf{R}_{\mathrm{eff}}|\Phi_1(g)\rangle|^2$$
$$=Ng(\nu)|\langle\varphi'|\mathbf{r}|\varphi\rangle|^2\Delta\nu. \tag{8.12}$$

The summation is restricted to states where the energy difference lies between $\hbar\nu\pm\frac{1}{2}\hbar\Delta\nu$. The left-hand expression is simply the sum over all the possible transitions, while the right-hand side defines $g(\nu)$. The theorem of spectroscopic stability assures that $\int_0^\infty g d\nu=1$ as required by (8.5).

The development is quite formal and gives no information regarding the shape and width of g. These are the required steps, however, to introduce the factor properly into the theory of optical absorption. It shows that the upper level widens.

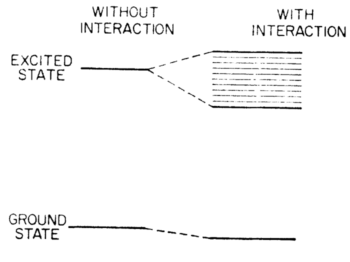

FIG. 5. Schematic diagram showing the effect of the interaction between centers.

This development indicates why one would not expect sharp lines in the absorption spectra of solids, except when one "imperfection" is very well shielded from another. Hence the absence of sharp lines in the spectroscopy of solids is to be expected (see the edge emission of CdS K2a, p. 117). This factor also accounts for the fact that the F center absorption does not have a fine structure. Unfortunately, we are unable to estimate the width of g, or to separate this broadening from the one caused by dispersion (K5).

It is assumed that g is wider than $\hbar\omega$, where ω is an effective phonon angular frequency. The g function is next replaced by the Dirac δ function. To obtain the moments, we integrate over many such functions. For the shape calculation, more care has to be used. On introducing the δ function into (8.3) and recalling items (1a) and (1b), we obtain

$$s(\nu)=b(4\pi^2/3)(e^2/\hbar c)\nu|\{\langle\Psi'(A)|\mathbf{r}|\Psi(A)\rangle\}|^2$$
$$\times\delta\{\nu-(1/\hbar)(E'-E)\}I_\nu. \tag{8.13}$$

The dimensions of s_{atomic} and $s(\nu)$ are not the same. s_{atomic} has the dimensions of ml^2t^{-3} (m for mass, l for length, and t for time). This arises because I_ν has the dimension of mt^{-2}, not energy per l^2t. Equation (8.3) assumes implicitly a δ function (S2, p. 215). In (8.13) we have written the δ function explicitly; hence $s(\nu)$ has the dimensions of ml^2t^{-2}.

The absorption cross section per imperfection in cm^2 is defined by

$$\frac{\text{energy absorbed per unit time in interval } \Delta\nu}{\text{energy falling on imperfection per unit time for unit area in interval } \Delta\nu}$$

or

$$\sigma(\nu)=b(4\pi^2/3)(\nu e^2/\hbar c)|\{\langle\Psi'(A)|\mathbf{r}|\Psi(A)\rangle\}|^2$$
$$\times\delta\{\nu-(1/\hbar)(E'-E)\}. \tag{8.13a}$$

This cross section must be summed over all the point imperfections in unit volume. Before summing (8.13a) we must consider the probability of finding a given imperfection with energy E. This is given by (B, p. 178)

$$P(v_t)=\Pi^j p(v_j), \tag{8.14}$$

where

$$p(v_j)=e^{-v_j\beta}(1-e^{-\beta_j})$$
$$=2e^{-(v_j+\frac{1}{2})\beta_j}\sinh\tfrac{1}{2}\beta_j \tag{8.14a}$$

and

$$\beta_j=\hbar\omega_j(g)/k\theta. \tag{8.14b}$$

The time average absorption constant is $\sum_{v,v'}P(v_t)\cdot\sigma(\nu)$. To obtain the actual measured absorption coefficient, the δ function must be eliminated. This can be done by the integration

$$\alpha_\omega=\frac{1}{\omega}N\int_{\nu-\frac{1}{2}\omega}^{\nu+\frac{1}{2}\omega}\sum_{v,v'}P(v_t)\sigma(x)dx. \tag{8.15}$$

On averaging $\sigma(\nu)$, the error of replacing g by δ is eliminated. For the calculation of the moments, one need not use (8.15) but simply integrate $\sum_{v,v'}P(v_t)\sigma(\nu)$ over many narrow "lines."

To carry the solution further, the delta functions must be expressed in terms of integrals. ν appears in the δ function and as a multiplier of this function. If the oscillator strength[‖‖] is introduced (S4),

$$f(\mathbf{R})=(2/3)(m/\hbar)\nu|\langle\varphi'(\mathbf{R})|\mathbf{r}|\varphi(\mathbf{R})\rangle|^2. \quad (8.16)$$

α_ω takes the following form

$$\alpha_\omega(\nu)=\frac{1}{\omega}bN\int_{\nu-\frac{1}{2}\omega}^{\nu+\frac{1}{2}\omega}d\nu\left[\frac{2e^2\pi^2}{cm}\sum_{v,v'}P(v_t)|\{\chi'|f^{\frac{1}{2}}|\chi\}|^2 \times\delta\left\{\nu-\frac{1}{\hbar}(E'-E)\right\}\right], \quad (8.17)$$

which nicely hides the frequency dependence of the term in front of the δ function. The mass of the electron (m) is introduced by using (8.16). It can be considered as an adjustable parameter provided we have a knowledge regarding the behavior of f. The next step is to forget about f's dependence on ν and $\mathbf{R}$ and write[¶¶]

$$\alpha_\omega(\nu)=\frac{2\pi^2be^2}{c\omega m}fN\int_{\nu-\frac{1}{2}\omega}^{\nu+\frac{1}{2}\omega}G(x)dx \quad (8.18)$$

$$G_n(\nu)=\sum_{v,v'}P(v)|\{\chi'|\chi\}|^2\delta\{\nu-(1/\hbar)(E'-E)\}. \quad (8.18a)$$

In Sec. 10 we shall show that G_n is normalized. In (8.18) the shape and moments only depend on the χ's. The assumption that f is independent of $\mathbf{R}$ is known as the Condon approximation. Meyer has eliminated this restriction. There is no good theoretical justification for the steps taken in obtaining (8.18). The frequency spread may be large over the bands, and one can hardly replace ν by an "average" value. In emission, a ν^3 appears before the δ function, and it certainly cannot be ignored. For instance, from the data on the emission from the F center in KCl at 77°K (D3) we know that $\epsilon_r(em)=1.08$ ev and $\epsilon_v(em)=1.35$ ev. Since $(1.25)^3=2$, the frequency factor could lead to an experimentally detectable skewness. One can assume that f is a function of the q's and of ν and still solve the moments problem. The present absorption data are not good enough to justify these added complications; they are considered only in Appendix V.

The theoretical problem is to know whether to treat $|\langle\varphi'(\mathbf{R})|\mathbf{r}|\varphi(\mathbf{R})\rangle|$ or $|\langle\varphi'(\mathbf{R})|\mathbf{p}_j(e)|\varphi(\mathbf{R})\rangle|$ as the fundamental quantity independent of the frequency. The sum rules are in terms of the f (S4, p. 503). Dirac's formulation of the radiation problem deals with matrix elements of $\mathbf{p}_j(e)$, while the elementary theory uses the matrix elements of the electron displacement. To refine the theory, this problem must first be resolved. This has not be done so far.

One cannot simply borrow theorems which hold for atoms since the phonon modes give additional degrees of freedom to the problem and their effects on the sum rules have to be explored with care.

Peierls, many years ago (S2, p. 671), considered the absorption problem when the centers have a lattice geometry. In this case the $\Phi_1(u,k)$'s have a rather simple form and strict selection rules exist for the transitions. The problem here has only an indirect relation to the one considered by Peierls. We assume a random distribution of imperfections; hence, no strict selection rules.

Lax and Burstein (L2a) have formulated the above in an alternate manner. They consider H_1 as a perturbation which broadens the Ψ's making bands out of the ground and excited states. This is an interesting and useful point of view.

Although there are limitations on (8.18a) we shall now use it to obtain the absorption coefficient when the ϵ_{jj}'s equal zero (Sec. 9), and the distribution moments in the most general case (Sec. 10). The foregoing equations apply rigorously to all the models discussed in the general introduction.

9. SHAPE OF THE BAND

Using a development of O'Rourke and Pekar, the integral $G_n(\nu)$ can be evaluated giving expressions for α. The problem, however, has to be simplified by the use of two assumptions: (1) that $\epsilon_{jj}=0$, and (2) that an effective mean frequency exists. Use is made of Mehler's formula and various expansions of the modified Bessel function.

The delta function can be expressed in the integral form (H3, p. 66)

$$\delta(\nu)=\frac{1}{2\pi}\int_{-\infty}^{\infty}e^{-i\nu t}dt. \quad (9.1)$$

By substituting (8.14a) and (9.1) into (8.18a), one obtains

$$G_n(\nu)=\frac{1}{2\pi}\int_{-\infty}^{\infty}e^{-i(\nu-\nu_{ug})t}\Pi^jF_j(t)dt, \quad (9.2)$$

where

$$F_j=2\sinh\tfrac{1}{2}\beta_j\int\int[\textstyle\sum_{v_j}\exp[-(v_j+\frac{1}{2})\lambda_j]\chi_j(q_j)\chi_j(q_j')] \times[\textstyle\sum_{v_j'}\exp[-(v_j'+\frac{1}{2})\mu_j]\chi_j'(Q_j)\chi_j'(Q_j')]dq_jdq_j' \quad (9.3)$$

$$\nu_{ug}=(1/\hbar)[\epsilon_u(\theta)-\epsilon_g(\theta)] \quad (9.3a)$$

$$\lambda_j=\beta_j+i\omega_jt \quad (9.3b)$$

and

$$\mu_j=-i\omega_jt. \quad (9.3c)$$

[‖‖] $\langle\varphi'|\mathbf{r}|\varphi\rangle$ is assumed to be real; thus $f^{\frac{1}{2}}$ is real. This allows a simplification in the notation without any limitation on the derived equations.

[¶¶] Since the absorption is small, we may assume that n is independent of ν (B5).

To obtain (9.3) we have employed (3.9), (3.24), (8.1a), and (8.2a). Also, a term has been added and subtracted in the exponent to make the next step simpler. μ_j arises from (9.1), while λ_j is a result of a combination of (9.1) and (8.14a). Finer mathematical points, such as the use of (9.1) and the rearrangement of the order of the summation will not be considered.

O'Rourke now uses Mehler's formula which can be written

$$\sum\nolimits_{v_j} e^{-(v_j+\frac{1}{2})\xi}\chi_j(q_j)\chi_j(q_j') \\ =\alpha_j(2\pi \sinh\xi)^{-\frac{1}{2}} \exp\{-\tfrac{1}{4}\alpha_j^2[(q_j+q_j')^2 \tanh\tfrac{1}{2}\xi \\ +(q_j-q_j')^2 \coth\tfrac{1}{2}\xi]\}, \quad (9.4)$$

where

$$\alpha_j^2=\omega_j/\hbar \quad (9.4a)$$

(Appendix III). The substitution of (9.4) into (9.3) makes the integrand take the simple form, $\exp[-ax^2+b]$. The operation can now be carried out by the use of standard formula, giving

$$F_j=\exp\left\{\frac{-\epsilon_j^2}{\omega_j^2(\omega_j\hbar)[\coth(\frac{1}{2}\beta_j+\frac{1}{2}i\omega_jt)-\coth\frac{1}{2}i\omega_jt]}\right\} \\ =\exp\left\{-\left(\frac{\epsilon_j^2}{2\omega_j^3\hbar}\right)[\coth\tfrac{1}{2}\beta_j-i \sin\omega_jt \\ -\coth\tfrac{1}{2}\beta_j \cos\omega_jt]\right\}. \quad (9.5)$$

The steps between (9.3) and (9.5) are essentially elementary, although slightly involved. The use of Mehler's formula does not require that the frequency of the two states be equal. One may obtain more general expressions for the F_j's [Vasileff (V1), or Dexter (D1)]. We want to obtain $\alpha_\omega(\nu)$, hence must obtain a rather simple expression for Π_jF_j. This is the reason for requiring that all the ϵ_{jj} vanish.

Now

$$\Pi^jF_j=\exp\left\{\sum\nolimits_j-\tfrac{1}{2}\left(\frac{\epsilon_j^2}{\hbar\omega_j^3}\right) \\ \times(\coth\tfrac{1}{2}\beta_j-i \sin\omega_jt-\coth\tfrac{1}{2}\beta_j \cos\omega_jt)\right\}. \quad (9.6)$$

The existence of the following equality (for any θ and t) must be assumed

$$\sum\nolimits_j\left(\frac{\frac{1}{2}\epsilon_j^2}{\hbar\omega_j^3}\right)[\coth\tfrac{1}{2}\beta_j-i \sin\omega_jt-\coth\tfrac{1}{2}\beta_j \cos\omega_jt] \\ =[\coth\tfrac{1}{2}\beta-i \sin\omega t-\coth\tfrac{1}{2}\beta \cos\omega t] \sum\nolimits_j \frac{\frac{1}{2}\epsilon_j^2}{\hbar\omega_j^3}. \quad (9.7)$$

The relation certainly holds for the CC and Fröhlich's model. If the local modes cluster about a point between the acoustical and optical branches, (9.7) should be a good approximation. One would not expect (9.7) to hold if the important modes are a combination of several types (longitudinal optical and local) involving radically different frequencies. Combined with (8.14b), it defines the "effective" or "average" frequency ω. In Sec. 11 a method is described which can be used to determine whether or not several effective frequencies exist. For the time being, (9.7) is used. Introducing the famous Huang and Rhys factor, we write

$$G_n(\nu)=\frac{1}{2\pi}\int_{-\infty}^{\infty} dt\, e^{-i(\nu-\nu_{ug})t} \\ \times\exp\{-S[\coth\tfrac{1}{2}\beta-i \sin\omega t-\coth\tfrac{1}{2}\beta \cos\omega t]\}, \quad (9.8)$$

where

$$S=\tfrac{1}{2}\sum\nolimits_j\frac{\epsilon_j^2}{\omega_j^3\hbar}=\sum\nolimits_j\frac{1}{\omega_j\hbar}\tfrac{1}{2}\omega_j^2(Q_j-q_j)^2, \quad (9.8a)$$

S is nondimensional. Equation (9.8) resembles integrals which appear in the definition of Bessel's function. To relate G_n to these functions, the following transformation is introduced:

$$\eta=(1/2)i\beta. \quad (9.9)$$

The integration variable of (9.8) is now changed to

$$x=\omega t-\eta. \quad (9.10)$$

Since one may show, with the use of (9.9) and (9.10) that

$$i \sin\omega t+\coth\tfrac{1}{2}\beta \cos\omega t=\operatorname{csch}\tfrac{1}{2}\beta \cos x, \quad (9.11)$$

Eq. (9.8) takes the form[***]

$$G_n(\nu)=\frac{1}{2\pi}\int_{-\infty}^{\infty}\frac{dx}{\omega}\exp\{-i(p\eta+px) \\ -S \coth\tfrac{1}{2}\beta+S \operatorname{csch}\tfrac{1}{2}\beta \cos x\}, \quad (9.12)$$

where

$$p=(\nu-\nu_{ug})/\omega. \quad (9.13)$$

One may show that[†††]

$$\frac{1}{2\pi}\int_{-\infty}^{\infty}\exp\{y \cos\xi-ip\xi\}d\xi=\sum_{-\infty}^{\infty}\delta(p-k)I_p(y), \quad (9.13a)$$

where I_p is the modified Bessel function and k is an integer. Now (9.12) takes the form

$$G_n(\nu)=\frac{e^{-ip\eta-S \coth\frac{1}{2}\beta}}{\omega}\sum_{-\infty}^{\infty}\delta(k-p)I_p[S \operatorname{csch}\tfrac{1}{2}\beta]. \quad (9.14)$$

[***] In (9.12) an alternate path of integration is used. This can be justified by taking contour integrals and assuming that p is an integer.

[†††] To establish (9.13) one must use an integral expression for I_n (J1, p. 547), and it is noted that $\delta(x)=\sum_{-\infty}^{\infty} e^{2\pi inx}$ for $-\frac{1}{2}<x<\frac{1}{2}$, etc.

Equation (9.14) requires that p or $(1/\omega)\sum_j \omega_j(v_j'-v_j)$ be an integer for any value of v_j and v_j'. This means that $\omega=\omega_j$. Evidently Eq. (9.7), which holds for any t, can only be satisfied under this condition. Therefore, the derivation holds exclusively for this condition.

The author believes that this is the result of using the δ function in Eq. (8.13) and that in reality Eq. (9.14) will give the correct shape (envelope—see Fig. 4) even if the frequencies vary over a small range. We thus write

$$p=v_t'-v_t. \tag{9.15}$$

Equation (9.14) can be put in the alternate form

$$G_n(\nu)=\left[\frac{\bar{v}+1}{\bar{v}}\right]^{p/2}\frac{1}{\omega}\exp[-S(2\bar{v}+1)]$$
$$\times\sum_k\delta(k-p)I_p\{2S[\bar{v}(\bar{v}+1)]^{\frac{1}{2}}\}, \tag{9.16}$$

where $\bar{v}=\frac{1}{2}[\coth(\beta/2)-1]$, the mean quantum number of a normal mode in the ground state.

The actually observed shape is obtained from (8.18); hence,

$$\frac{1}{\omega}\int_{\nu-\frac{1}{2}\omega}^{\nu+\frac{1}{2}\omega}G_n(\nu)d\nu=\frac{1}{\omega}\left[\frac{\bar{v}+1}{\bar{v}}\right]^{p/2}$$
$$\times\exp[-S(2\bar{v}+1)]I_p\{2S[\bar{v}(\bar{v}+1)]^{\frac{1}{2}}\}, \tag{9.17}$$

where p is the integer closest to $(1/\omega)(\nu-\nu_{ug})$. ω appears in (9.17) because the unknown g function has been effectively replaced by the step function.

$$g=0 \quad \text{for} \quad \nu<\frac{1}{\hbar}(E'-E)-\tfrac{1}{2}\omega$$
$$g=\frac{1}{\omega} \quad \text{for} \quad \frac{1}{\hbar}(E'-E)-\tfrac{1}{2}\omega\leq\nu\leq\frac{1}{\hbar}(E'-E)+\tfrac{1}{2}\omega \tag{9.18}$$
$$g=0 \quad \text{for} \quad \frac{1}{\hbar}(E'-E)+\tfrac{1}{2}\omega<\nu.$$

The factor $1/\omega\exp[-S(2\bar{v}+1)]$ does not affect the frequency dependence of the absorption, i.e., the shape. It is convenient to introduce an average shape factor

$$G_A=\left[\frac{\bar{v}+1}{\bar{v}}\right]^{p/2}I_p\{2S[\bar{v}(\bar{v}+1)]^{\frac{1}{2}}\}. \tag{9.19}$$

The term $1/\omega$ is a measure of the width of the band. Larger ω's cause wider absorption bands provided that the ϵ_j's remain the same. We shall see that $\int_{-\infty}^{\infty}e^{-S(2\bar{v}+1)}G_A dp=1$ so that $\int G_n(\nu)d\nu=1$ (Appendix IV and Sec. 10).

Equation (9.19) is exact for the models considered provided (9.7) applies. It does not require that $\epsilon_j\rightarrow 0$. This is not obvious unless the derivation of O'Rourke is used. Two alternate forms of G_A will now be found using some developments originally due to Pekar (P1).

(a) Low Temperature

If $\theta\rightarrow 0$, $\bar{v}$ is a small quantity. It is useful to define $z=2S[\bar{v}(\bar{v}+1)]^{\frac{1}{2}}$ which is also a small quantity. Here $v_t\rightarrow 0$, and $p>0$; hence, our concern is for the situation where p is a positive integer. Now we expand I_p as follows (J1, p. 542):

$$I_p(z)=\frac{(\frac{1}{2}z)^p}{p!}\left[1+\frac{(\frac{1}{2}z)^2}{p+1}+\frac{(\frac{1}{2}z)^4}{2(p+2)(p+1)}+\cdots\right] \tag{9.20}$$

and obtain

$$G_A(\nu)\approx G_l(\nu)=S^p/p!. \tag{9.21}$$

This approximation improves as p increases. For large S, one may use the Stirling approximation and show that the maximum occurs at

$$p_l=S. \tag{9.22}$$

This corresponds to the angular frequency

$$\nu_l=\nu_{ug}+S\omega. \tag{9.22a}$$

Since p is an integer, S in (9.22) refers to the nearest integer value. The violet side of the band corresponds to higher values of p, where (9.21) is a better approximation.

It seems appropriate to refer to (9.21) by the name Pekarian, since Pekar was the first to employ expansion (9.20) in relation to this problem. The use of Eq. (9.21) requires the inequality,

$$z^2/4p\ll 1. \quad \text{(Pekarian Criterion)} \tag{9.23}$$

At the point of maximum absorption this is equivalent to the conditions

$$S\bar{v}\ll 1. \tag{9.24}$$

The shape of the absorption band of some F centers seems to be given by (9.21) (K4). Little is known about this type of curve. Its behavior is studied in Appendix IV.

(b) High Temperature

At high temperatures $\bar{v}$ is not small and $z\gg 1$. As the temperature increases, z approaches the value $2Sk\theta/\hbar\omega$. This suggests the use of the asymptotic expansion‡‡‡

$$I_p(z)=\frac{e^z}{(2\pi z)^{\frac{1}{2}}}\left\{1+\sum_{n=1}^{\infty}\frac{(-1)^n[4p^2-1][4p^2-3^2]\cdots[4p^2-(2n-1)^2]}{n!(8z)^n}\right\}. \tag{9.25}$$

---

‡‡‡ This type of expansion is discussed by Jeffreys and Jeffreys (J1). Their equation for I_p, however, is slightly in error.

Our interests are not limited to small values of p or to the first few terms of the sum. p may have the value of 100; hence, for appropriate values of z the major contribution arises from terms with high values of n. If the series can be broken off before $r \approx p$, the simple form is obtained,

$$I_p(z) = \frac{e^z}{(2\pi z)^{\frac{1}{2}}} \left\{ 1 - \frac{p^2}{2z} + \frac{1}{2!}\left(\frac{p^2}{2z}\right)^2 - \frac{1}{3!}\left(\frac{p^2}{2z}\right)^3 + \cdots \right\}$$

$$= \frac{1}{(2\pi z)^{\frac{1}{2}}} \exp\left(z - \frac{p^2}{2z} \right). \tag{9.26}$$

For (9.26) to hold, one requires that $(2n-1)^2 \ll 4p^2$ for all important terms. This will be true if $p^2/2z < 1$. When $p^2/2z > 1$, the expansion (9.26) must be explored further. The highest terms of the series occur (approximately) at $n = p^2/2z$, or Eq. (9.26) requires that $4p^2 > (p^4/z^2)$. These facts suggest that criteria for the applicability of (9.26) are

$$|2z/p| > 1 \tag{9.27a}$$

and (Gaussian criteria)

$$|p| \gg 1. \tag{9.27b}$$

The high-temperature shape is obtained by substituting (9.26) in (9.19),

$$G_A(\nu) \approx G_h(\nu)$$

$$= \frac{1}{(2\pi z)^{\frac{1}{2}}} \exp\left\{ z - \frac{1}{2z} p^2 + \frac{p}{2} \ln\left(1 + \frac{1}{\bar{v}}\right) \right\}. \tag{9.28}$$

Its maximum occurs at

$$p_h = \tfrac{1}{2} z \ln\left(1 + \frac{1}{\bar{v}}\right) = \frac{\hbar\omega}{2k\theta} z \tag{9.29}$$

$$\approx S \tag{9.29a}$$

and

$$\nu_h = \nu_{ug} + (\hbar\omega^2/2k\theta) z \tag{9.30}$$

$$\approx \nu_{ug} + S\omega. \tag{9.30a}$$

The peak value of G_h is

$$G_h(\max) = \frac{1}{(2\pi z)^{\frac{1}{2}}} \exp\left\{ z\left(1 + \frac{\hbar^2\omega^2}{8k^2\theta^2}\right) \right\}. \tag{9.31}$$

Hence

$$G_h = G_h(\max) \exp\left\{ -\frac{1}{2}\left(\frac{p}{\sqrt{z}} - \frac{\hbar\omega}{2k\theta}\sqrt{z} \right)^2 \right\} \tag{9.32}$$

$$= G_h(\max) \exp\left\{ -\frac{1}{2z\omega^2} (\nu - \nu_h)^2 \right\}. \tag{9.32a}$$

Thus at high temperatures the absorption should be Gaussian provided (9.27a) and (9.27b) apply.

TABLE III.

θ °K	$\bar{v}$	$\frac{4k\theta}{\hbar\omega}$	$\frac{[\bar{v}(\bar{v}+1)]^{\frac{1}{2}}}{\theta}$	z for $S=30$
5	3.11×10^{-13}	0.139	1.11×10^{-7}	3.34×10^{-5}
10	5.58×10^{-7}	0.278	7.47×10^{-5}	4.48×10^{-2}
20	7.47×10^{-4}	0.555	1.36×10^{-3}	1.63
30	8.30×10^{-3}	0.834	3.04×10^{-3}	5.47
50	5.95×10^{-2}	1.39	5.02×10^{-3}	15.1
75	0.172	2.08	5.96×10^{-3}	26.8
100	0.311	2.78	6.40×10^{-3}	38.4
200	0.949	5.56	6.80×10^{-3}	81.6
400	2.31	11.1	6.91×10^{-3}	165.
600	3.69	16.7	6.93×10^{-3}	250.
800	5.07	22.2	6.96×10^{-3}	334.

If the ϵ_j's do not approach zero, p will be greater than unity, and criterion (9.27b) will hold, except in the region where $p=0$, i.e., $\nu = \nu_{ug}$. Since $p_h > 0$, this occurs to the red of the peak. In the broad bands which arise in polar solids, this will not be a real limitation on the applicability of (9.32a).

To test criterion (9.27a) at the peak, it is combined with (9.29) to give

$$2z/p_h = 4k\theta/\hbar\omega > 1. \tag{9.33}$$

In Table III some typical values of $\bar{v}$, z, $(4k\theta/\hbar\omega)$ and $(1/\theta)[\bar{v}(\bar{v}+1)]^{\frac{1}{2}}$ are given. The phonon frequency selected was $2\pi(3\times10^{12})$ sec^{-1} (M5). The table indicates that (9.33) applies above room temperature. Since $p < p_h$ for the red side of the band, Eq. (9.23a) should hold there.

If we multiply G_h by $(1/\omega)\exp\{-S(2\bar{v}+1)\}$ one sees that $\int G_n d\nu = 1$, provided one neglects small quantities. In the next section we show that this relation holds exactly.

Deviation from a Gaussian form should be looked for on the violet side of the peak where $p > p_h$; here (9.27b) could break down. This treatment does not suggest that a band should be Gaussian for all ν, although at medium temperatures one would suspect that the red side would approach such a shape. At some temperatures the following conditions may occur: $(2z/p) > 1$ for the red side (Gaussian), and $(z^2/4p) < 1$ on the violet side (Pekarian).

We may obtain an expression for H at high temperatures. Equations (7.7) and (9.32a) show that $2\hbar^2\omega^2 z = 1/a^2$ and

$$H = (5.545)^{\frac{1}{2}} \hbar\omega z^{\frac{1}{2}}$$

$$= (5.545)^{\frac{1}{2}} S^{\frac{1}{2}} \hbar\omega \operatorname{csch}^{\frac{1}{2}} \tfrac{1}{2}\beta. \tag{9.34}$$

For high θ

$$H = (11.090 S k \hbar\omega)^{\frac{1}{2}} \theta^{\frac{1}{2}}. \tag{9.34a}$$

Equation (9.30) predicts that the peak of the absorption band is temperature dependent. The dependence is given by $\nu_{ug}(\theta)$ and z/θ. In Table III the dependence of $[\bar{v}(\bar{v}+1)]^{\frac{1}{2}}/\theta$ on θ is given. This quantity is proportional to z/θ of (9.30). Except at low temperatures, where our approximations break down, this term is insensitive to variations of θ.

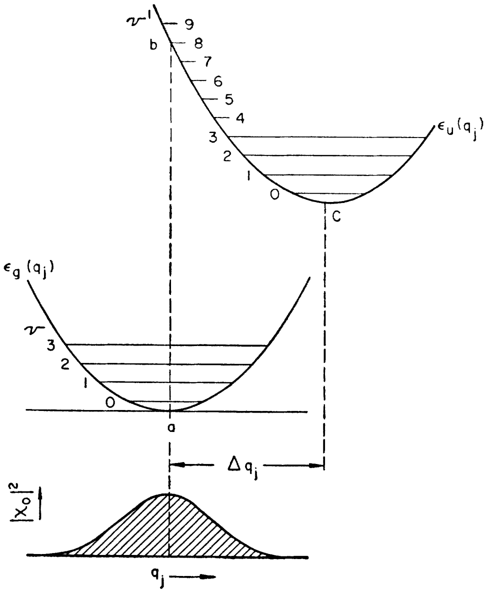

FIG. 6. Diagram illustrating the broadening effect. The upper and lower configurational coordinates are shown. The distribution probability at 0°K is given in the lower left corner. Point "a" is at $\epsilon_g(\mathbf{R}_g)$, while "c" is at $\epsilon_u(\mathbf{R}_u)$.

The dependence of ν_h and H on temperature given by (9.30) and (9.34) is due to the approximations used in this section. These relations require correction, but the high-temperature prediction is valid and (9.34a) holds.

The physical interpretation of the above equations is indicated in Fig. 6. Although the development considers more than one mode, this description is limited to the CC model. This is done for convenience only, as the arguments can be generalized to any number of effective modes. Since the ϵ_{jj}'s are zero, the frequencies are not affected by the transition. In Fig. 6 $\epsilon_g(q)$ and $\epsilon_u(q)$ are plotted against q. The horizontal lines are various values of $E=\epsilon_g+\hbar\omega(v+\frac{1}{2})$ and $E'=\epsilon_u+\hbar\omega(v'+\frac{1}{2})$. The relative probability of finding a particular value of q, when the electron is in the ground state, is shown by the shaded area on the lower left. The probable distribution, $\rho(q)$, at absolute zero is $\chi^2(q)$ for $v=0$. At any finite temperature it is

$$\rho(q)=\sum_v p(v)\chi^2(q)=\frac{1}{a\sqrt{\pi}}\exp[-q^2/a^2], \tag{9.35}$$

where

$$a=\left(\frac{\hbar}{\omega}\right)^{\frac{1}{2}}\coth^{\frac{1}{2}}\tfrac{1}{2}\beta. \tag{9.35a}$$

One obtains (9.35) from (8.14a) and (9.4). At high temperatures a^2 has the value $2k\theta/\omega^2$, and (9.35) has a form which one can obtain by Boltzmann's statistics if the total energy of the system is assumed to be $(1/2)\omega^2q^2$. The actual energy of the system, however, is not $(1/2)\omega^2q^2$, since (9.35) is the sum over many states unless $\theta=0$°K.

The first question is: what is S? It is simply the ratio of the difference in potential energy at 0 (b) and at Δq (c) to the energy of a phonon, $\hbar\omega$ (Fig. 2). This follows from (3.24) and (9.8a). The maximum of the absorption occurs for transitions from $v=0$ to $v'=S$ as is seen with the use of (9.22) and (9.29a). This is the vertical transition if we ignore the zero-point energy. One would expect this to be the peak because of the shape of $\rho(q)$. So far complex analysis has not led to anything very surprising.

The bandshape at low temperature, however, is non-Gaussian; indeed it is nonsymmetric. This means that $|\{\chi_{S+1}'|\chi_0\}|^2$ does not equal $|\{\chi_{S-1}'|\chi_0\}|^2$. Here 0 and $S\pm 1$ refer to the quantum states of χ and χ'. This lack of symmetry leads to the skewness in absorption curves at low temperatures. This has created a serious problem in the experimental analysis (K2a, p. 119). We stress that this lack of symmetry stems from the properties of the χ's and not $\epsilon_u(q)-\epsilon_g(q)$, which for this problem has the simplest form possible, namely

$$\hbar\nu=\hbar\nu_{ug}+\tfrac{1}{2}\omega^2(\Delta q)^2-\omega^2(\Delta q)q. \tag{9.36}$$

ν is a *linear* function of q.

At high temperatures the spread on the red side occurs because of transitions where $v_t'-v_t$ is smaller than S. The violet side is affected by transitions from the ground state where v_t' is greater than S. The theory suggests that these transitions tend to make the curve more symmetrical and in the extreme case, Gaussian.

The Williams' approximation suggests that the transition probability at frequency ν is obtained from (9.35) and (9.36). First, (9.36) is solved for q; then the absorption is obtained from $\rho(q)$. Since $\rho(q)$, however, is composed of several states (unless $\theta=0$°K), this approach is inconsistent, since $\epsilon_u(q)-\epsilon_g(q)$ does not equal $E'-E$. Further, the matrix elements are somewhat asymmetrical.

The question of the asymmetry of the absorption band is an extremely fundamental one. The Williams' approximation happens to give the correct temperature dependence of H (Sec. 10). Equation (9.34) might also be a good approximation. Actually, it is a poor one. It is the asymmetry of the curves, i.e., Eq. (9.21), which gives us the necessary insight to understand what is really happening.

In conclusion, one should mention that Krivoglaz and Pekar (K5) report a shape where the term $\text{const}(\nu-\nu_h)^3$ is added to the expression in the curly brackets of Eq. (9.32a). This term will create a skewness when $(\nu-\nu_h)$ is not too small. As ν approaches ν_h, the curve becomes symmetric and almost Gaussian. This fits the experimental data better than (9.32a), since there is another adjustable parameter. The experimental data seems to resemble a double Gaussian curve more nearly, however. There is no evidence, however, to believe that a discontinuity in the absorption occurs at $\nu=\nu_h$.

Arguments by Kubo and Toyozawa (K6) indicate that the simple model employed here gives a symmetrical shape at high temperatures. This same conclusion can be obtained from the higher moments calculated by O'Rourke. The conclusion of Sec. 9(b) regarding the symmetry of the shape is not due to (9.25). Experimental data suggests (K4) that the results may not be completely valid. However, the simplifying assumptions give some useful information regarding the low-temperature shape and the transition probabilities.

10. METHOD OF MOMENTS

The method of moments was developed by Lax (L1) and extended by Meyer (M8). We now combine the development of Part I with this powerful approach.

Returning to Eq. (8.13a), we first sum over v_t' and then take a weighted average over v_t using (8.14); thus,

$$\alpha(\nu)=\frac{K}{2\pi}\operatorname{Av}\int_{-\infty}^{\infty}\sum\nolimits_{v'}dt\{\chi|f^{\frac{1}{2}}|\chi'\}\{\chi'|f^{\frac{1}{2}}|\chi\}$$

$$\times\exp\left\{i\left[(E'-E)\frac{1}{\hbar}-\nu\right]t\right\}, \quad (10.1)$$

$$K=2\pi^2be^2N/cm. \quad (10.1a)$$

In this approach $\alpha(\nu)$ is used. To obtain (10.1) we have made use of (9.1). Av implies a weighted average over the ground vibrational states. By expanding $\exp\{iE't/\hbar\}$ in series, one may show that

$$\chi'\exp\{iE't/\hbar\}=e^{iH_ut/\hbar}\chi'. \quad (10.2)$$

Now (10.1) takes the form

$$\alpha(\nu)=\frac{K}{2\pi}\operatorname{Av}\int dt\sum\nolimits_{v'}$$

$$\times\{\chi|f^{\frac{1}{2}}e^{iH_ut/\hbar}|\chi'\}\{\chi'|f^{\frac{1}{2}}e^{-iH_gt/\hbar}|\chi\}e^{-i\nu t}. \quad (10.3)$$

We note that E' depends on v_t'; H_u, however, does not. Therefore, we take it out of the sum. Equation (10.3) is a product of the three integrals: one over t; the other over the nuclear coordinates involved in the first { }; while the third arises because of the second { }. Since the χ's form a complete set in q space, we use the following property of eigenfunctions (H3, p. 66)

$$\sum\nolimits_{v_j'}\chi_j'(q_j)\chi_j'(q_j')=\delta(q_j-q_j') \quad (10.4)$$

and write

$$\alpha(\nu)=\frac{K}{2\pi}\int dt\operatorname{Av}\{\chi|f^{\frac{1}{2}}e^{iH_ut/\hbar}f^{\frac{1}{2}}e^{-iH_gt/\hbar}|\chi\}e^{-i\nu t}. \quad (10.5)$$

Now the Condon approximation is used to remove f from the matrix element, giving

$$\alpha(\nu)=\frac{Kf}{2\pi}\operatorname{Av}\int dt\{\chi|e^{i(H_u-H_g)t/\hbar}|\chi\}e^{-i\nu t}. \quad (10.6)$$

The quantum mechanics is contained in the order of the operators; thus one cannot remove $\exp\{i(H_u-H_g)t/\hbar\}$ from the matrix (Appendix V).

By assuming that f is frequency independent, we see that α is the Fourier transform of the function $Kf\operatorname{Av}\{\chi|\exp[i(H_u-H_g)t/\hbar]|\chi\}$ and it follows that (M7, p. 252)

$$Kf\operatorname{Av}\{\chi|e^{i(H_u-H_g)t/\hbar}|\chi\}=\int\alpha(\nu)e^{i\nu t}d\nu. \quad (10.7)$$

Setting $t=0$, we find

$$\int\alpha(\nu)d\nu=Kf. \quad (10.8)$$

Therefore, it follows that $G_n(\nu)$ of (8.18a) is normalized. The thermal vibration spreads the absorption band but does not affect the area. Equation (10.8) is based on the approximation that f is *independent* of frequency. Had we assumed that $\langle\varphi'|\mathbf{r}|\varphi\rangle$ is frequency dependent, the zero moment would be temperature sensitive. Using (7.1), it follows that

$$M_0=\hbar Kf. \quad (10.9)$$

Further,

$$\left\{(\hbar/i)(\partial/\partial t)\int\alpha(\nu)e^{i\nu t}d(\hbar\nu)\right\}_{t=0}=\int\alpha(\nu)\hbar\nu d(\hbar\nu)$$

$$=(\hbar^2/i)Kf\operatorname{Av}[(\partial/\partial t)\{\chi|e^{i(H_u-H_g)t/\hbar}|\chi\}]_{t=0} \quad (10.10)$$

and

$$M_1=\hbar Kf\operatorname{Av}\{\chi|H_u-H_g|\chi\}. \quad (10.10a)$$

Now,

$$\left\{-\hbar^2\frac{\partial^2}{\partial t^2}\int\alpha(\nu)e^{i\nu t}d(\hbar\nu)\right\}_{t=0}=\int(\hbar\nu)^2\alpha(\nu)d(\hbar\nu) \quad (10.11)$$

and

$$M_2=\hbar Kf\operatorname{Av}\{\chi|(H_u-H_g)^2|\chi\}. \quad (10.14)$$

By similar methods we may evaluate the higher moments. For these situations, one may not write

$$\exp\{(i/\hbar)(H_u-H_g)t\}$$

for

$$\exp\{(i/\hbar)H_ut\}\exp\{(-i/\hbar)H_gt\}$$

as explained in Appendix V.

To evaluate (10.10) and (10.12), expressions for the operator H_u-H_g as well as $\operatorname{Av}\{\chi|q_j^n|\chi\}$ (n is an integer) are required. The matrix elements can be calculated from the properties of the χ's and are (B, p. 173–181)

$$\mathrm{Av}\{\chi|q_j|\chi\}=0 \tag{10.13a}$$

$$\mathrm{Av}\{\chi|q_j^2|\chi\}=[\hbar/2\omega_j(g)]\coth\tfrac{1}{2}\beta_j \tag{10.13b}$$

$$\mathrm{Av}\{\chi|q_j^3|\chi\}=0 \tag{10.13c}$$

$$\mathrm{Av}\{\chi|q_j^4|\chi\}=3[\hbar/2\omega_j(g)]^2\coth^2\tfrac{1}{2}\beta_j. \tag{10.13d}$$

β_j is defined by (8.14b) where the ground state ω_j is used.

An expression for (H_u-H_g) is obtained from (8.1), (8.2) and the expansion technique employed in Sec. 3. It now follows that

$$H_u-H_g=\Delta\epsilon(\theta)+\sum_j\epsilon_jq_j+\tfrac{1}{2}\sum_j\epsilon_{jj}q_j^2 +\tfrac{1}{2}\sum_{jk}{}'\,\epsilon_{jk}q_jq_k \tag{10.14}$$

$$\Delta\epsilon(\theta)=\epsilon_u(\mathbf{R}_g)-\epsilon_g(\mathbf{R}_g)=\hbar\nu_{ug}+\tfrac{1}{2}\sum_j\epsilon_j^2/\omega_j^2(u). \tag{10.14a}$$

To obtain (10.14) and (10.14a) use has been made of (3.27). When comparing Secs. 9 and 10, it should be remembered that $\Delta\epsilon$ does *not* equal $\hbar\nu_{ug}$. The prime on the sum means that $j\neq k$. The temperature dependence of $\Delta\epsilon$ is due to the expansion of the crystal. We assume that the ϵ_j's and ϵ_{jk}'s are independent of θ. The derivatives are evaluated at the equilibrium position of the ground state, and the q_j's are the normal modes for this state.

The evaluation of M_1 and M_2 is now straightforward. Using (10.9) and (10.10)

$$\bar{\epsilon}=(M_1/M_0) =\Delta\epsilon(\theta)+\tfrac{1}{4}\sum_j\epsilon_{jj}[\hbar/\omega_j(g)]\coth\tfrac{1}{2}\beta_j. \tag{10.15}$$

To evaluate M_2 we square (10.14), i.e.,

$$\begin{aligned}(H_u-H_g)^2=\Delta\epsilon^2(\theta)&+\sum_j\epsilon_j^2q_j^2+\sum_{jk}{}'\,\epsilon_j\epsilon_kq_jq_k\\&+\tfrac{1}{4}\sum_j\epsilon_{jj}^2q_j^4+\tfrac{1}{4}\sum_{jk}{}'\,\epsilon_{jj}\epsilon_{kk}q_j^2q_k^2\\&+2\Delta\epsilon(\theta)\sum_j\epsilon_jq_j+\Delta\epsilon(\theta)\sum_j\epsilon_{jj}q_j^2\\&+\Delta\epsilon(\theta)\sum_{jk}{}'\,\epsilon_{jk}q_jq_k\\&+\sum_{jk}\epsilon_j\epsilon_{kk}q_jq_k^2,\end{aligned} \tag{10.16}$$

where again terms involving $\epsilon_j\epsilon_{kl}$ and $\epsilon_{ij}\epsilon_k\epsilon_l$ $(k\neq l)$ have been omitted. Using (10.12) and (10.13) results in

$$\begin{aligned}(M_2/M_0)=\Delta\epsilon^2(\theta)&+\sum_j[\hbar/2\omega_j(g)]\epsilon_j^2\coth\tfrac{1}{2}\beta_j\\&+\tfrac{1}{8}\sum_j\epsilon_{jj}^2[\hbar^2/\omega_j^2(g)]\coth^2\tfrac{1}{2}\beta_j\\&+\tfrac{1}{16}\sum_{jk}\epsilon_{jj}\epsilon_{kk}[\hbar^2/\omega_j(g)\omega_k(g)]\coth\tfrac{1}{2}\beta_j\coth\tfrac{1}{2}\beta_k\\&+\tfrac{1}{2}\Delta\epsilon(\theta)\sum_j\epsilon_{jj}[\hbar/\omega_j(g)]\coth\tfrac{1}{2}\beta_j.\end{aligned} \tag{10.17}$$

A combination of (7.3), (10.15), and (10.17) gives the important equation

$$m^2=\sum_j\epsilon_j^2[\hbar/2\omega_j(g)]\coth\tfrac{1}{2}\beta_j +\tfrac{1}{8}\sum_j\epsilon_{jj}^2[\hbar^2/\omega_j^2(g)]\coth^2\tfrac{1}{2}\beta_j. \tag{10.18}$$

We have made only two assumptions—that f is not a function of ν or q, and that the adiabatic approximation can be used to terms of ϵ_{ij}, ϵ_{kl}, and $\epsilon_j\epsilon_{kl}$, where $k\neq l$.[§§§] These equations are extremely general. The possibility of calculating the q's and ϵ's about a point imperfection with any degree of accuracy is small. Hence, the equations as they stand are of little use. We must make further assumptions to obtain relations between $\bar{\epsilon}$, m, and θ which involve parameters to be evaluated experimentally. The generality of the equations assures one that terms will not be omitted. Thus, we may apply the equations to the Huang-Rhys problem (the Fröhlich approximation) and compare our results with those of O'Rourke and Meyer. On the other hand, we may make the approximation used by Klick.

(a) CC Model

Here, there is only one q whose ground state has the angular frequency $\omega(g)$; hence, from Sec. 3,

$$X=q/M^{\frac{1}{2}}, \tag{10.19}$$

where M is an effective mass of the order of an ionic mass. For this model

$$\begin{aligned}\Delta\epsilon(q)&=\hbar\nu_{ug}+\tfrac{1}{2}\omega^2(u)(q-\Delta q)^2-\tfrac{1}{2}\omega^2(g)q^2\\&=\hbar\nu_{ug}+\tfrac{1}{2}\omega^2(u)(\Delta q)^2-\omega^2(u)(\Delta q)q\\&\quad+\tfrac{1}{2}[\omega^2(u)-\omega^2(g)]q^2.\end{aligned} \tag{10.20}$$

Using the definition of (3.18),

$$\epsilon_j=-\omega^2(u)\Delta q=-\omega^2(u)M^{\frac{1}{2}}\Delta X \tag{10.21a}$$

and

$$\epsilon_{jj}=\omega^2(u)-\omega^2(g)\approx2\omega(g)\Delta\omega. \tag{10.21b}$$

Equations (10.15) and (10.18) now have the form

$$\bar{\epsilon}=\Delta\epsilon(\theta)+\tfrac{1}{2}\hbar\Delta\omega\coth\tfrac{1}{2}\beta \tag{10.22a}$$

and

$$m^2=\left\{\frac{1}{2}\frac{\omega^2(u)}{\hbar\omega(g)}M(\Delta X)^2\right\}\hbar^2\omega^2(u)\coth\tfrac{1}{2}\beta \times+\tfrac{1}{2}\hbar^2(\Delta\omega)^2\coth^2\tfrac{1}{2}\beta. \tag{10.22b}$$

A generalized S is defined by the use of (10.18) and (10.22b),

$$S=\frac{1}{2\hbar}\sum_j\epsilon_j^2\frac{1}{\omega_j(g)\omega_j^2(u)}=\tfrac{1}{2}\sum_j\frac{\omega_j^2(u)}{\hbar\omega_j(g)}(Q_j-q_j)^2. \tag{10.23}$$

The last step uses (3.24). S equals the expression in the curly brackets of (10.22b). This definition agrees with (9.8a) and is equivalent to the one used by Meyer. An exact comparison is somewhat involved since Meyer takes a thermal average over modes which do not include V_I and V_e of (5.2). The S for absorption and emission need not be the same. Both $\omega(g)$ and $\omega(u)$ enter into the definition.

[§§§] We also assume that the modes are nondegenerate (Sec. 3).

The second term in (10.22b) is new; it arises from a superior approximation.[‖‖‖] To estimate its effect we set $\theta=0$°K and $\Delta\omega\approx\omega$. Now

$$m_0=\hbar\omega[S+(1/2)]^{\frac{1}{2}}$$
$$=\hbar\omega S^{\frac{1}{2}}[1+(1/4S)]. \qquad (10.22c)$$

If S is of the order of 30, the correction term is of the order of 0.01, which is at the experimental limit of accuracy. If S were smaller than 30, and if $\Delta\omega$ is large, one might be able to detect the second term in (10.22b). This would be done from the temperature behavior of m.

Equation (10.22a) has a great deal less information than (10.22b), since no reliable information regarding $\Delta\epsilon(\theta)$ exists. As stated, $\Delta\epsilon$ may change because of the lattice expansion. ϵ_m for the F center seems to be a function of the interionic distance, d. From empirical data, one may obtain the following relation, $\epsilon_m(d)=\text{const}\, d^{-1.84}$ (Mollwo (M10), Ivey (I1)). Combining this with density measurements at various temperatures, one may calculate $\Delta\epsilon(\theta)$. Using Henglein's (H3a) expansion data for KCl, one obtains

$$\epsilon_m(193°\text{K})-\epsilon_m(273°\text{K})=0.011 \text{ ev}$$
$$\epsilon_m(80°\text{K})-\epsilon_m(273°\text{K})=0.025 \text{ ev},$$

where $\bar{\epsilon}$ has been replaced by ϵ_m. This change of ϵ_m is too small to explain the observed temperature variation (0.040 ev and 0.070 ev), which is an indication that $\Delta\omega\neq 0$ for this particular absorption band. One might attempt to combine the Ivey relation with (10.22a).

On the other hand, we may assume that $\Delta\epsilon(\theta)$ equals a constant. This can be tested by plotting ϵ_m against $\coth\beta/2$; β having been evaluated empirically from (10.22b). If the data give the equation $A+B\coth\beta/2$, one may evaluate $\Delta\epsilon$ and $\Delta\omega$. There is a danger in this procedure since $\Delta\epsilon(\theta)$ may also vary as $A+B\coth\beta/2$ over a limited range of temperatures [for small β, $\coth\beta/2\approx(2/\beta)$]. In this situation the coefficient of $\coth\beta/2$ would not equal $\frac{1}{2}\hbar\Delta\omega$. As the range of θ increases, the possibility of accidental correlation decreases.

Using recent data on the F center in KCl, ω has been evaluated with the use of (10.22b) (without the second term). From (10.22a) ω, $\bar{\epsilon}$, and $\hbar\Delta\omega$ were determined. One again concludes that the correction to (10.22b) is very small.

Klick and Schulman (K2a, p. 110) have used the Williams' approximation to obtain an expression for H. It is identical to the first term of (10.22b), provided H and m are proportional. This does not imply that the derivation given here is identical to the one obtained previously. The latter method does not give the second term of Eq. (10.22b), nor the Pekarian shape (at low temperature). The latter is readily observable and requires understanding. If one uses Eq. (9.34), H depends on the $\operatorname{csch}\beta/2$ instead of $\coth\beta/2$, which indicates that the relation given by William and Hebb (W3) and by Lax (L2) is fortuitous.

(b) Huang-Rhys Problem

In this case we assume that all the modes have a single frequency given by the LST relation; then

$$\bar{\epsilon}=\Delta\epsilon(\theta)+\tfrac{1}{2}\textstyle\sum_j \hbar\Delta\omega_j \coth\tfrac{1}{2}\beta \qquad (10.24a)$$

and

$$m^2=\hbar^2\omega^2(u)S\coth\tfrac{1}{2}\beta+\tfrac{1}{2}(\textstyle\sum_j \hbar^2\Delta\omega_j^2)\coth^2\tfrac{1}{2}\beta. \qquad (10.24b)$$

Equation (10.24a) was first obtained by O'Rourke, using the approximation that $\Delta\omega$ is *very* small. Later Meyer obtained this equation by an alternate method. These authors did not note the thermal dependence of $\Delta\epsilon(\theta)$. The first term of Eq. (10.24b) has been given before, while the second term is new, see however (K6). It may be detected when careful measurements are made on bands with small S's.

(c) Double-Frequency Model

We may apply (10.15) and (10.18) to more complex situations. An alternate model is one with two effective ground frequencies ω_1 and ω_2. For this situation

$$\bar{\epsilon}=\Delta\epsilon(\theta)+\frac{\hbar}{4\omega_1(g)}\{\textstyle\sum_j\epsilon_{jj}\}\coth\tfrac{1}{2}\beta_1$$
$$+\frac{\hbar}{4\omega_2(g)}\{\textstyle\sum_i\epsilon_{ii}\}\coth\tfrac{1}{2}\beta_2 \qquad (10.25a)$$

and

$$m^2=\hbar^2\omega_1^2(u)S_1\coth\tfrac{1}{2}\beta_1+\hbar^2\omega_2^2(u)S_2\coth\tfrac{1}{2}\beta_2. \qquad (10.25b)$$

Here

$$S_1=\tfrac{1}{2}\textstyle\sum_j[1/\hbar\omega_j(g)\omega_j^2(u)]\epsilon_j^2 \qquad (10.26a)$$
$$S_2=\tfrac{1}{2}\textstyle\sum_i[1/\hbar\omega_i(g)\omega_i^2(u)]\epsilon_i^2 \qquad (10.26b)$$
$$\beta_1=(\hbar/k\theta)\omega_1(g) \quad\text{and}\quad \beta_2=(\hbar/k\theta)\omega_2(g). \qquad (10.26c)$$

j is summed over the modes associated with the frequency ω_1, and i is over the ω_2 modes. The second term in (10.18) is omitted.

We again use an effective frequency and write

$$S_1=[1/2\hbar\omega_1(g)\omega_1^2(u)]\textstyle\sum_j\epsilon_j^2. \qquad (10.27)$$

Since the data are always limited to a range in temperature, this may be less restrictive than (9.7) which must hold for every value of t. If (10.27) is to hold for every value of β_j, there cannot be a spread in the values of the ω's.

We may assume that S_1 is related to the local modes, and S_2 is associated with the longitudinal optical modes. β_1 will be roughly half β_2. The question is: can one detect the difference between (10.25a and b) and (10.22a and b) or (10.24a and b)? For the answer to this question, we must consider the various methods employed to analyze the data.

[‖‖‖] A term of this nature appears in the formal treatment of Kubo and Toyozawa (K6).

11. ANALYSIS OF EXPERIMENTAL DATA

In the last two sections, we derived several equations which can be compared with experimental data. Various attempts have been made to analyze the data with radically different results. Some of the difficulties stem from the data itself, yet this is not the major problem. While at low temperatures (Table I) there is considerable disagreement, this is not the case at room temperature (Table IV). The agreement between Mollwo's (M10) and the most recent data (M5) is good. Russell and Klick's (R1) value of H seems to be too large at all temperatures.

Russell and Klick conclude that (10.22b) (without the second term) applies to the F center, provided the angular frequency in KCl is 1.6×10^{13} sec^{-1}. On the other hand, Pekar (P2 and 4) and Meyer (M8 and 9) conclude that the same equation holds, provided a value of 3.95×10^{13} sec^{-1} is used. It was obtained from the LST relation. Pekar and Meyer use Mollwo's data. The reason for the difference stems from the method of treating the data. One may use Mollwo's data with an alternate method of analysis and obtain 2×10^{13} sec^{-1} for ω.

Pekar's analysis is most remarkable (P4, p. 129 ff and p. 145 ff). He had only one adjustable constant, the effective mass of the electron. It was evaluated from the experimental ϵ_m at room temperature; hence, his results should apply to the most recent data. Using this value, Pekar calculated S by employing (9.8a) and (3.18a). For the relation between the q's and the X's he used the very long wave approximation (B, p. 213). His value of S for KCl is 23.8. Using this value, the LST relation (10.24b), and (7.7b), we compute the values in Table V. Equation (7.7b) was used to relate m and H; this gives

TABLE IV. F center in KCl at room temperature.

Experimenter	(M10)	(R1)	(M5)
ϵ_m ev	2.20	2.2	2.225
H ev	0.35	0.39	0.35

$$H^2=8\ln2(\hbar\omega)^2\coth\tfrac{1}{2}(\hbar\omega/k\theta).\tag{11.1}$$

The calculation of H at 300°K does not agree with the value, 0.40, reported in Pekar's paper of 1950 since it was based on Eq. (9.34), not (10.24b). Strangely enough, in 1953 Krivoglaz and Pekar (K5) derived (11.1). However the corrected numerical values of H were not reported in Pekar's subsequent review paper (P3), although (11.1) was quoted. The correct expression for H at 0°K seems to have been first given by Pekar in 1950 (P1). While the results of the table are not satisfactory, they are really quite remarkable, since there is only *one* adjustable parameter.

A method of analysis which the author believes is quite useful is now discussed. If one has to use Eqs. (10.15) and (10.18) with various values of β_j, the problem becomes hopeless since the number of adjustable parameters is too large. The opposite point of view, which is very naive, is that one exists and that Eqs. (10.22a) and (10.22b) or (10.24a) and (10.24b) apply. If we further assume that $\Delta\epsilon$ is independent of temperature, there are only four adjustable parameters and the equations of interest take the forms[¶¶¶]

TABLE V. Comparison of Pekar's parameters with experiment.

θ	H (cal)	H (exp)
300°K	0.43	0.35
0°K	0.30	0.16

$$\bar{\epsilon}=\Delta\epsilon+B\coth\tfrac{1}{2}(\hbar\omega/k\theta)\tag{11.2}$$

$$m^2=\hbar^2\omega^2S\coth\tfrac{1}{2}(\hbar\omega/k\theta)+\tfrac{1}{2}B^2\coth^2\tfrac{1}{2}(\hbar\omega/k\theta).\tag{11.3}$$

Next we may assume that B^2 is very small compared to $\hbar^2\omega^2S$ and hence can be omitted from (11.3). This is true for the F center in KCl. To obtain m from an arbitrary curve is a laborious process involving a great deal of numerical work. In some cases, one may be able to replace m by H [Eqs. (7.7b) and (7.12b)], hence in the simplest situation we wish to test critically the relation

$$H^2=H^2(0)\coth\tfrac{1}{2}(\hbar\omega/k\theta),\tag{11.4}$$

where $H(0)$ is the half-width at 0°K. It can readily be obtained from measurements at low temperatures (approx 4°K). The validity of (11.4) is based on the assumption that the ratio of m to H is temperature independent. This has to be tested by numerical integration.

Equation (11.4) suggests plotting $\coth^{-1}[H/H(0)]^2$ against $1/\theta$. We have the desired test if $1/\theta$ can be varied over a large range of values. A straight line going through the origin is a clear indication of the validity of (11.4) and the development in Sec. 10. Further, it shows that there is one effective mode, so the theory developed in Sec. 9 can be used. Such a plot is a more critical test of the theory than the previous methods of analysis, since one deals with straight lines rather than a complex curve. If one combines this technique of analysis with Mollwo's data, one obtains the 2×10^{13} sec^{-1} value mentioned above.

Three alternate methods have been suggested.

(1) Klick (K2) plots H against $\theta^{\frac{1}{2}}$. At high temperatures, a straight line is obtained whose slope is proportional to $S^{\frac{1}{2}}\omega^{\frac{1}{2}}$. At moderately low temperatures, a departure from a straight line is obtained and the analysis requires the determination of this departure. At extremely low temperatures (about 25°K), one gets a straight horizontal line. While Klick's approach is useful, one cannot determine the validity of (11.4) in a

---

[¶¶¶] We assume here that $(\Sigma_j\hbar\Delta\omega_j)^2=\Sigma_j(\hbar\Delta\omega_j)^2$ which, of course, need not be true except in the CC model. The B from (11.2) will however give us the order of magnitude of B^2 in (11.3).

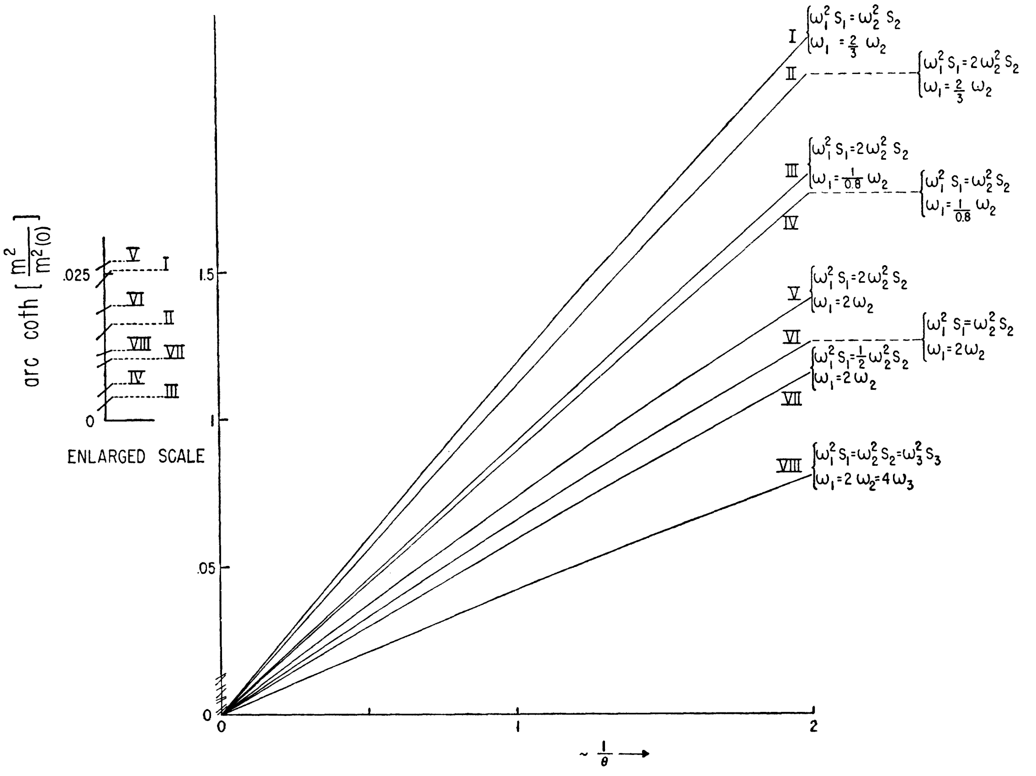

FIG. 7. Broadening caused by more than one effective frequency. Note the curve at $1/\theta = 0$. In some cases m can be replaced by H. Analysis of more than one ω.

critical manner since the points are not supposed to lie on a straight line.

(2) Pekar (P3) has plotted H against θ. In this case one does not get a straight line except at extremely low temperatures. An analysis of experimental data by this method is difficult, and the author knows of no detailed study using this approach.

(3) Meyer (M8) has plotted $(H/\hbar\omega)^2$ against $\coth\frac{1}{2}(\hbar\omega/k\theta)$ using a known ω (from the LST relation). An erroneous ω can be detected only at low temperatures (under 100°K). If a great many points are available below 100°K, one can see that his technique does not give a straight line except for the correct value of ω. Thus, using recent data on the F center in KCl (M5) one may show that his ω is incorrect. Mollwo's data had too few points in the critical region, so that Meyer was unable to detect the deviation. Actually, Meyer was unable to confirm (11.4) and was forced to add a constant [Appendix V and Eq. (11.5)].

We are particularly interested in what happens when there is a breakdown in the approximation made in arriving at (11.4). In particular, how does Eq. (10.25b) look on a plot of $\coth^{-1}[H^2/H^2(0)]$ against $1/\theta$? This question is only meaningful provided the ratio of ω_1 to ω_2 is not near unity, and S_1 and S_2 are approximately equal. One cannot hope to detect the difference between Eqs. (10.25b) and (11.4) with the use of experimental data unless there is an appreciable contribution from both types of modes, and the frequencies are distinct. One may assume that both the local modes and the longitudinal optical modes interact with the trapped electron. The local modes should be in the gap between the acoustical and optical branches. In NaCl and KCl this gap is roughly at one-half the frequency of the longest longitudinal optical modes; hence the ratio of the ω's should be of the order of 2.

To understand the problem various $\coth^{-1}[H(\theta)/H(0)]^2$ against $1/\theta$ plots have been made using several ratios of S_1 to S_2 and several ratios of ω_1 to ω_2 (Fig. 7).**** In making these graphs, the values of S_1, S_2, ω_1, and ω_2 were assumed to be known. Then, $H^2(\theta)$ was calculated. From this H^2, $\coth^{-1}[H^2(\theta)/H^2(0)]$ was computed. Since the data refer only to a limited range of temperatures, the curvature shown in Fig. 7 will not be detected. A sure indication of the difference between (11.4) and (10.25b) is in the intercept, where $1/\theta = 0$. If the line goes through the origin, we have a fair experimental proof that (11.4) applies, and that there is a *single effective* frequency. If not, one must attempt to express H by means of a more complete equation. Strangely enough, the data on the F center in KCl can be interpreted in this very simple manner (K4).

Similarly, in Fig. 8 plots have been made with the use of Meyer's equation, namely,

$$H^2 = C + D \coth\tfrac{1}{2}(\hbar\omega/k\theta). \qquad (11.5)$$

This equation assumes that $f^{\frac{1}{2}}$ is a linear function of q

---

**** In Figs. 7 and 8 we assume that $m \approx H$.

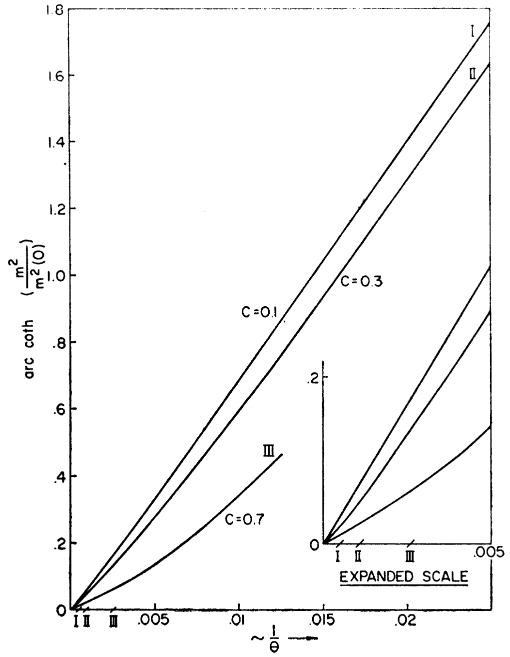

FIG. 8. Broadening effects when $f^{\natural}$ is a linear function of q. Note the curve at $1/\theta=0$ [in Eq. (11.5) D is set equal to unity]. In some cases m can be replaced by H.

(Appendix V). Again, the same conclusion is obtained; namely, the validity of (11.5) can be judged by the interception at $1/\theta=0$.

Use of this kind of plot requires measurements at both low and high temperatures. Measurements at extremely low temperatures cannot be used, since $H^2/H^2(0)$ approaches unity, and there is a large uncertainty in the $\coth^{-1}$ of $H^2/H^2(0)$ due to slight uncertainty in the evaluation of H^2 (one or two parts per thousand). This is one disadvantage of this plot. The other proposed methods are no better in this temperature region if (11.4) applies.

As suggested by Meyer, one may test (11.2) by plotting $\bar{\epsilon}$ or ϵ_m against $\coth\frac{1}{2}(\hbar\omega/k\theta)$, ω having been determined from (11.4). If $\Delta\epsilon$ is independent of θ one will obtain a straight line. Of course, $\Delta\epsilon$ could vary as const$+b$ $\coth\beta/2$ for a limited range of θ.

No completely satisfactory method suggests itself for testing the shape of an absorption band, since we do not have a simple analytic relation between α and ϵ. It is fairly well established that (7.7) and (7.8) will not apply to absorption bands in solids, except in very special cases. For detailed comparison of the theory and experiment, see the forthcoming paper (K4).

12. CONCLUSIONS OF PART II

The theory developed in the first sections is applied to an impurity center with two bound states. Considerations are limited to absorption and, for a large part, to the simplest model (Secs. 9, 11, and 17). It has thus been possible to make exact calculations.

The broadening of an absorption band is on account of at least several causes. The band is composed of narrow subbands. The width of these arises from the uncertainty principle, from the center-center interaction, and from the dispersion of the normal modes. The envelope curve (the height of the subbands) is due to the displacement of the normal modes during an optical transition. The over-all shape arises from terms which appear in phonondynamics and are absent in electrodynamics. The broadening effects are illustrated in Fig. 9. The energy levels of the system are drawn on the left-hand side. At absolute zero before the transition, the system is in its ground state ($v_t=0$). Various transition probabilities exist for the excitation to levels in the excited state ($v_t'=0, 1, 2, \cdots$). The height of the vertical lines on the right are proportional to these transition probabilities (Eq. 9.21). The result is an asymmetric curve which resembles the F center in KCl (K4). We have plotted v_t' from right to left as is usually done. For emission one may exchange v_t and

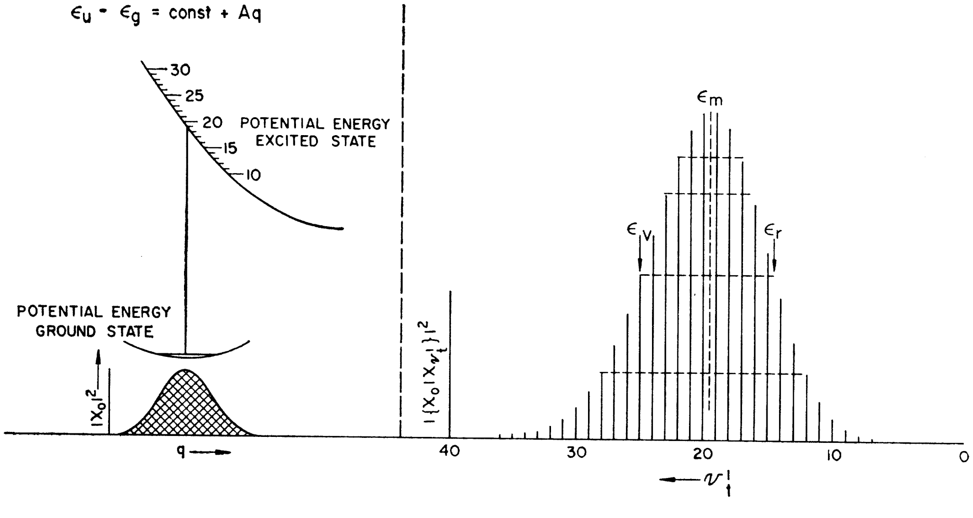

FIG. 9. Band shape at $\theta=0°$K for $S=20$. The vertical lines on the right are proportional to the transition probability. Note $\epsilon_v-\epsilon_m>\epsilon_m-\epsilon_r$ and the lack of symmetry for all values of α.

v_t'. Here the emitted energy is $\Delta\epsilon(Q=0)-\hbar\omega(v_t-v_t')$, and the diagram should be "flipped over." The absorption curve shown on the right is probably not limited to the model on the left but only requires that all the important normal modes (whose ϵ_j do not equal zero) have an effective single frequency (Sec. 9). The generalization of Fig. 9 to any model with a single effective frequency is a result of the use of Mehler's formula. This is a result of the fundamental contribution of O'Rourke.

The shape presented is thus exact for the model considered at absolute zero. To extend these calculations to higher temperatures, various approximations must be made. The asymmetry disappears and the agreement with experiment is much less good. One may indeed show rigorously that the model on the left of Fig. 9 gives a symmetrical curve at high temperatures. This can be done most simply by calculating the third moment (01). Hence the model has to be expanded to predict the shape observed at high temperatures in the F center of KCl (K4).

As to the accuracy of the theory developed, the simple model (Sec. 9) does not predict the correct relation between E^e and E^a. For example, in the F center of KCl, $S=30$, $\hbar\omega=0.012$ ev, and E^a (at 0°K)$=2.3$ ev. From (4.2a), $E^e=E^a-2\hbar\omega S=1.6$ ev compared to the experimental value of 1.2 ev (V1). For this situation we may not let the frequency change be zero, and a more complex calculation is required (Sec. 10). For large values of S, we do not have to describe the potential curve over the entire range if we are interested only in emission or in absorption shapes. Returning to Fig. 2, the absorption shape is determined primarily by the potential curves about points "a" and "b." Likewise the emission shape also is determined primarily from the curves about "c" and "d." Therefore, one would expect that the general features given in Sec. 9 will be observed. While the general features are given by the development, the calculations are not truly exact. The change in the frequency and higher-order terms must have a detectable influence. These corrections must somehow be used to explain the asymmetry at high temperatures. How to do this remains an unsolved problem.

In Secs. 10 and 18 several more general models are considered where various corrections are introduced in the expression for the moments. The effects on $\bar{\epsilon}$ and m^2 are, however, small and usually beyond the range of detection, except for the case where we have two radically different frequencies. We thus conclude that the basic equations have considerable validity. This field needs more reliable data and its complete analysis in terms of absorption and emission. In Sec. 11 some methods of analysis are suggested.

ACKNOWLEDGMENTS

Professor F. Seitz is thanked for suggesting that this review be written and for several helpful discussions. The assistance of Dr. A. Ellett in writing the manuscript is acknowledged. Further, the author is grateful to J. D. Konitzer for carrying out a detailed experimental investigation of the shape and thermal behavior of the F center in KCl. The author also thanks Mrs. B. Heckenbach for typing the manuscript.

Note added in proof.—Some interesting recent data have been reported by K. Maeda, J. Phys. Soc. Japan **14**, 478 (1959).

13. APPENDIX I. LIST OF SYMBOLS

Although an attempt was made to associate a single physical concept with every symbol, this has not always been possible; thus, ϵ has been used for an eigenvalue as well as for a photon energy. Similarly, m has two distinct meanings. Usually subscripts have been employed to differentiate between physical concepts, or the symbols have been employed at distinct parts of the text. Gaussian units have been employed except for experimental values which are reported in electron volts. Only the important symbols are listed here.

a_s—Smakula's constant—ratio of the area under an absorption curve to the product of $\alpha_m H$; also $(G_m H)^{-1}$
b—local field correction (Sec. 8)
c—velocity of light
e—charge on the electron
f—oscillator strength (8.16)
g—shape factor associated with items (a) and (b) of Sec. 7, as well as the dispersion of the modes
$\hbar$—Planck constant divided by 2π
h_e—electronic Hamiltonian (3.3)
h_v—vibration Hamiltonian (3.4)
k—Boltzmann constant
(k)—the kth nuclei
m—See (7.3) except (8.16)
q_j—reduced coordinate of the jth normal mode (In Part II it is associated with the ground state.)
Δq_j—shift in the equilibrium position $q_j'-Q_j$ (3.24)
p—see (9.13)
p_l—see (9.22)
p_h—see (9.29)
p_j—momentum operator associated with q_j
$\mathbf{r}$—coordinate of all the electrons of interest to the problem
t—kinetic energy operator associated with the excess electron
v_j—vibration quantum number associated with the jth mode, v_j (ground), and v_j' (upper)
v_t—total vibrational quantum number, i.e., $\sum_j v_j$
$\bar{v}$—thermal average quantum number of single mode
B—reference (B2)
E—total energy in vibrational state v_t associated with the ground-electronic state
E'—total energy in vibrational state v_t' associated with the upper-electronic state

E^a—activation energy for absorption
E^e—activation energy for emission
E^t—thermal activation energy
G_A—see (9.19)
G_n—normalized shape factor associated with the absorption or emission of phonons
G_m—maximum value of G_n
H—width at half-height (half-width) (7.4)
H—total Hamiltonian [see (3.12), (3.13), (5.4), and (5.10) for various meanings]
K—see (10.1a)
LST—Lyddane-Sack-Teller relation (see B, p. 86)
M_n—nth moment of the absorption curve (7.1)
N—number of imperfections per unit volume
Q_j—reduced coordinate of the jth mode associated with the upper state
$P(v_t)$—see (8.14)
$\mathbf{R}$—coordinate of all the nuclei
$\mathbf{R}_L$—value of $\mathbf{R}$ which minimizes V_L
$\mathbf{R}_n$—see (3.4a)
S—Huang-Rhys factor $\frac{1}{2}\sum_j \epsilon_j^2/\hbar\omega_j^3$ (4.3a) and (10.23)
T—kinetic energy operator for all the nuclei
T'—T which only operates on the χ's
T_e—kinetic energy operator for all the electrons
V—total potential energy of the system
V_e—potential energy due to an excess electron
V_I—potential energy due to a point imperfection
V_L—potential energy of a perfect lattice
$X_\alpha(k)$—actual coordinate of the kth particle in the αth direction
α—absorption coefficient
α_m—absorption coefficient at ϵ_m
β_j—see (8.14b)
ϵ—stands for an eigenvalue
ϵ_g—ground state eigenvalue of h_e
ϵ_j—see (3.18a)
ϵ_{jk}—see (3.18b)
ϵ_n—nth eigenvalue of h_e
ϵ_u—upper state eigenvalue of h_e
ϵ_v—vibrational eigenvalue
$\Delta\epsilon(\mathbf{R}) = \epsilon_u(\mathbf{R}) - \epsilon_g(\mathbf{R})$—see after (5.3) for special meaning in Secs. 5(a) and 14
$\Delta\epsilon$ or $\Delta\epsilon(\theta) = \Delta\epsilon(\mathbf{R}_g)$ in Part II
ϵ—also stands for a photon energy
ϵ_m—photon energy for maximum absorption
$\bar{\epsilon}$—see (7.2)
θ—absolute temperature
ν—*angular* frequency of the absorbed light
ν_{ug}—see (9.3a)
σ—absorption cross section
φ—electronic eigenfunction [φ (ground) and φ' (upper) are also used]
χ_j and χ_j'—ground- and upper-state vibrational eigenfunctions associated with the jth mode
χ and χ'—total vibrational eigenfunctions of the ground and excited states
Ψ—total eigenfunction of the system
ω—the effective angular frequency of the interacting phonons
ω_j—angular frequency associated with the jth mode

14. APPENDIX II. MEYER-PEKAR METHOD

This appendix relates the method developed for the trapped electron (5a) to the techniques used previously. Meyer (M8) has made the most extensive calculation. We now split $H_0(A)$ of (5.2) as follows:

$$H_L = T' + V_L + V_I \tag{14.1}$$

$$H_e = t + V_e(\mathbf{R}_I) \tag{14.2}$$

and

$$H_{Le} = V_e(\mathbf{R}) - V_e(\mathbf{R}_I). \tag{14.3}$$

The division of H_0 here is not identical to the one made previously. Equation (14.1) determines a set of normal modes, Λ_j, from an expansion about the point defined by

$$\left[\frac{\partial}{\partial X_\alpha(k)}(V_L + V_I)\right]_{\mathbf{R}_I} = 0. \tag{14.4}$$

There is a close similarity [see Eqs. (3.12a) and (3.12b)] between $H_L + H_e$ and $H_0(S)$ and between H_{Le} and $H_1(S)$. The $H_0(S)$ and $H_1(S)$ here correspond to the impurity model of Sec. 5. The potential energy term in $h_v(\mathbf{R})$ has been modified slightly. Meyer refers to H_{Le} as the lattice-center interaction. This term is actually given by $H_1(A)$.

An appropriate way to find a solution is to expand H_{Le}, as follows,

$$H_{Le} = \sum_j a_j\Lambda_j + \tfrac{1}{2}\sum_{jk} b_{jk}\Lambda_j\Lambda_k. \tag{14.5}$$

We assume that the eigenfunctions φ_n and eigenvalues $\Delta\epsilon_n$ of H_e are known at $\mathbf{R}_I$. The perturbation method is now used to obtain eigenvalues and eigenfunctions of $H_e + H_{Le}$ for any $\mathbf{R}$. Thus,

$$\varphi_n(\mathbf{R}) = \varphi_n + \sum_j \sum_m{}' \frac{\langle\varphi_m|a_j|\varphi_n\rangle}{\Delta\epsilon_n - \Delta\epsilon_m}\varphi_m\Lambda_j + \text{higher terms}. \tag{14.6}$$

In the last term $m \neq n$, and we assume that the eigenvalues associated with H_e are nondegenerate. The argument $\mathbf{R}_I$ of φ and $\Delta\epsilon$ on the right-hand side of (14.6) has been omitted. The higher-order terms which are proportional to $\Lambda_j\Lambda_k$ arise from the use of second-order perturbation theory as well as from the last term of (14.5).

The $\varphi_n(\mathbf{R})$'s must form an orthogonal set with respect to $\mathbf{r}$ for a fixed value of $\mathbf{R}$. This follows since the complete series (14.6) gives eigenfunctions of the Hamiltonian $H_e + H_{Le}$. This was not evident to Meyer.

Associated with (14.6) is the eigenvalue

$$\Delta\epsilon_n(\mathbf{R})=\Delta\epsilon_n+\textstyle\sum_j\langle\varphi_n|a_j|\varphi_n\rangle\Lambda_j$$
$$+\tfrac{1}{2}\textstyle\sum_{jk}\langle\varphi_n|b_{jk}|\varphi_n\rangle\Lambda_j\Lambda_k$$
$$+\textstyle\sum_m{}'\sum_{jk}\dfrac{1}{\Delta\epsilon_n-\Delta\epsilon_m}\langle\varphi_n|a_j|\varphi_m\rangle\langle\varphi_m|a_k|\varphi_n\rangle\Lambda_j\Lambda_k. \quad (14.7)$$

Terms of (14.7) may be identified with those which arise in an expansion about $\mathbf{R}_I$. We assume proper convergence. In such an expansion, terms similar to those in (3.18) appear. Thus,

$$\epsilon_j=\langle\varphi_n|a_j|\varphi_n\rangle \quad (14.8a)$$

and

$$\epsilon_{jk}=\langle\varphi_n|b_{jk}|\varphi_n\rangle$$
$$+\textstyle\sum_m{}'\dfrac{1}{\Delta\epsilon_n-\Delta\epsilon_m}\langle\varphi_n|a_j|\varphi_m\rangle\langle\varphi_m|a_k|\varphi_n\rangle. \quad (14.8b)$$

Equation (14.8a) is a form of (3.16). The first term in (14.8b) was omitted by Meyer. One may use the ϵ_j's exactly as in Sec. 3 to determine the relation between the true q's and the Λ's. One should stress that H_{Le} does not arise from a true electron-phonon interaction but occurs only because a fictitious definition of the phonon field was used. On occasion the Λ's are assumed to have a very simple form, and the ϵ's obtained by these means correspond only very approximately with the real ones.

15. APPENDIX III. MEHLER'S FORMULA

Mehler's formula, Eq. (9.4), is "well known" in the theory of Hermite polynomials and has been used since it was discovered in 1866. Its proof is not available in standard texts. The steps are rather simple, providing one interchanges two integrals with an infinite sum. A proof due to Hardy is presented. It originally appears in a paper by Watson (W1). We shall not concern ourselves with the convergence of the series, so the proof as presented is not completely rigorous. A standard integral of interest is

$$\int_{-\infty}^{\infty}\exp[-a^2u^2+ibu]du=\frac{\sqrt{\pi}}{a}\exp[-b^2/4a^2]; \quad (15.1)$$

hence,

$$H_v=(-1)^v\exp[x^2]\frac{d^v}{dx^v}\exp[-x^2]$$
$$=\frac{(-2i)\exp[x^2]}{\sqrt{\pi}}\int_{-\infty}^{\infty}u^v\exp[-u^2+2ixu]du. \quad (15.2)$$

One would like to examine the sum

$$\sum_0^\infty t^v\chi_v(x)\chi_v(y)$$
$$=\textstyle\sum_v\dfrac{1}{2^v v!\sqrt{\pi}}\exp\{-\tfrac{1}{2}(x^2+y^2)\}t^vH_v(x)H_v(y)$$
$$=\pi^{-\frac{3}{2}}\exp\{\tfrac{1}{2}(x^2+y^2)\}\textstyle\sum_v\displaystyle\int\int\frac{(-2tuw)^v}{v!}$$
$$\times\exp\{-u^2-w^2+2ixu+2iyw\}dvdw. \quad (15.3)$$

For convenience, the usual $\omega/\hbar$'s which appear in the χ's have been omitted. v is the quantum state of χ_v. Hardy's device is to change the order of the sum and the integrals. Further, he replaces $\sum[(-2tuw)^v/v!]$ by $\exp\{-2tuw\}$. The convergence of (15.3) is such that this is permissible, provided $t^2<1$. Watson states this requirement but does not give details. One can see that (15.4) requires this relation. After this step, Eq. (15.1) is used twice, going from right to left. Thus,

$$\textstyle\sum_v t^{v+\frac{1}{2}}\chi_v(x)\chi_v(y)$$
$$=t^{\frac{1}{2}}\pi^{-\frac{3}{2}}\exp\{\tfrac{1}{2}(x^2+y^2)\}$$
$$\times\int\int_{-\infty}^{\infty}\exp\{-u^2-2tuw-w^2+2ixu+2iyw\}dudw$$
$$=t^{\frac{1}{2}}\pi^{-1}\exp\{\tfrac{1}{2}(x^2-y^2)\}$$
$$\times\int\exp\{-(1-t^2)u^2+2i(x-yt)u\}du$$
$$=\pi^{-\frac{1}{2}}\left[\frac{t}{1-t^2}\right]^{\frac{1}{2}}\exp\left\{\frac{x^2-y^2}{2}-\frac{(x-yt)^2}{1-t^2}\right\}$$
$$=\pi^{-\frac{1}{2}}\left[\frac{t}{1-t^2}\right]^{\frac{1}{2}}\exp\left\{-\frac{(x^2+y^2)}{2}\left(\frac{1+t^2}{1-t^2}\right)+xy\frac{2t}{1-t^2}\right\}. \quad (15.4)$$

If we set $t=e^\xi(\xi>0)$, Eq. (15.4) gives (9.4) after some elementary transformations which use the properties of the hyperbolic functions.

16. APPENDIX IV. PEKARIAN CURVE

Properties of Pekarian curves, Eq. (9.21), are discussed here. This equation gives the relative probability for a transition from $v_t=0$ to any $v_t'=p$ (Eq. 9.15). Since the number of modes does not enter into the problem, we again use the CC model as an illustration. The Pekarian shape is not limited to this case but also applies to the Fröhlich and LM models. The only serious limitation is the use of Eq. (9.7).

Absorption shapes do not seem to be completely symmetric (K2a, p. 118), and one may inquire as to the symmetrical properties of the Pekarian curve. Consider first the case where $S=20$. The most probable transi-

TABLE VI. The symmetry properties of a Pekarian curve $S=20$.

$p=v_t'$	23	22	21	20	19	18	17	16
$\frac{S^p}{p!}\left(\frac{S^S}{S!}\right)^{-1}$	$\frac{(20)^3}{(21)(22)(23)}$	$\frac{(20)^2}{(21)(22)}$	$\frac{20}{21}$	1	1	$\frac{19}{20}$	$\frac{19(18)}{(20)^2}$	$\frac{(17)(18)(19)}{(20)^3}$
Transition probability	0.7529	0.8658	0.9524	1	1	0.9500	0.8550	0.7268

tions occur for $v_t'=S-1$ and S. If one assumes that the transition probability for these jumps is unity, then one may obtain the properties in Table VI. The transition probabilities do not lie symmetrically about the midpoint, which is very nearly at 19.5.

To stress the asymmetry of the problem, Fig. 9 is included. The left-hand side is similar to Fig. 6 except that the upper state has been shifted twice as much, and only the case where $v_t=0$ is considered. On the right-hand side $|\{\chi'|\chi\}|^2$ is plotted against v_t'. On the x axis v_t' increases in going from right to left, in agreement with experimental procedure. It is evident that $\epsilon_v-\epsilon_m\neq\epsilon_m-\epsilon_r$ so that the Pekarian curve is asymmetric.

In Fig. 10 three Pekarian curves for $S=3$, 10, and 20 are plotted. On the curves the ratio of $\epsilon_v-\epsilon_m$ to $\epsilon_m-\epsilon_r$ is noted. These values show that the curve is slightly lopsided for all values of S and resembles a double Gaussian. The violet side is indeed almost a perfect Gaussian.

To calculate various factors associated with a Pekarian curve, we use (9.17) and let $\theta=0$. The following formula is obtained:

$$|\{\chi_p'|\chi_0\}|^2=Ge^{-s}=(S^p/p!)e^{-s}. \tag{16.1}$$

0 and p are the total vibrational quantum numbers of the states χ and χ'. The term $1/\omega$ has not been included. It determines the width (or height) of the curve. Also, we set $\omega=\hbar\omega=1$. Using (10.9) and (10.24b) we note that,

$$\textstyle\sum_{v_t'}|\{\chi'|\chi_0\}|^2=1 \tag{16.2}$$

and

$$m^2=S. \tag{16.3}$$

Since $M_0=1$ it is temperature independent [Eq. (10.9)]. Hence, we know that the relation

$$\textstyle\sum_{v_t}P(v_t)\sum_{v_t'}|\{\chi'|\chi_0\}|^2=1 \tag{16.4}$$

holds for any θ. Now, since

$$\textstyle\sum_{v_t}P(v_t)=1, \tag{16.5}$$

we conclude that

$$\textstyle\sum_{v_t'}|\{\chi'_{v_t'}|\chi_{v_t}\}|^2=1 \tag{16.6}$$

for any v_t. This is a sum-rule which has one surprising feature—it does not involve the frequency. In atomic spectra, the sum-rules involve the transition frequency. This means that we may not accept the atomic sum-rules without further careful considerations.

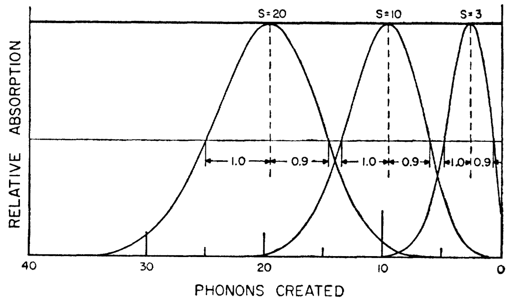

FIG. 10. Three Pekarian curves for various values of S. Note the lack of symmetry.

By numerical calculation we obtain Table VII. Here the lines of Fig. 9 have been replaced by the envelope curve. Column 3 is the value of the absorption at the peak (at p_l).†††† The fifth column is the area (planimeter) under the curves when the factor e^{-s} is included. This area might be slightly larger than unity because we are replacing a sum by a smooth curve. At $S-\frac{1}{2}$ the envelope is larger than the values at S or at $S-1$. To obtain the sixth column, use was made of (16.3), and the seventh is obtained from the definition of Smakula's constant found in Sec. 7, combined with (16.2). Columns 6 and 7 should be compared with the value found for the Gaussian shape, that is, 5.545 and 1.064. The Lorentzian value of a_s is 1.57. The deviation from the Gaussian values is very small. The variation for small values of S is probably real; however, we attach no importance to the slight deviation found in the last four rows. One may readily superimpose various Pekarian curves unless S is smaller than 10.

TABLE VII. Some properties of Pekarian curves.

S	p_l	$(e^{-s}G)_{\max}$	H	Area	$H^2/m^2=H^2/S$	$a_s(P)$
3	2.5	0.229	4.18	1	5.82	1.04
5	4.5	0.180	5.28	1.01	5.58	1.06
10	9.5	0.126	7.46	1.00	5.57	1.07
20	19.5	0.0892	10.56	1.01	5.58	1.07
30	29.5	0.0728	12.92	1.01	5.56	1.07

17. APPENDIX V. EFFECTS WHICH OCCUR WHEN f IS NOT A CONSTANT

We now consider what happens to the equations of Sec. 10 when the simplifying assumptions regarding f

---

†††† Since no fine structure is observed p will not be limited to integer values.

are removed. One might use the Lax-Meyer method throughout, but the algebraic complexities become too involved. In Sec. 10 we replaced $\exp(iH_ut/\hbar)\times\exp(-iH_gt/\hbar)$ by $\exp[i(H_u-H_g)t/\hbar]$. It is correct only to terms in $(H_u-H_g)^2$. This arises because $\exp(iH_ut/\hbar)$ is only a shorthand notation for an infinite series and the terms in the two sums do not in general commute. Hence, this method is not used in the first section of this Appendix.

The two problems are: what happens to the expression for $\bar{\epsilon}$ and m^2 when f becomes a linear function of the frequency, or a linear function of the q's?

(a) Oscillator Strength Depends on the Frequency

First, we consider the effects of having the oscillator strength proportional to the frequency. For this purpose, the dipole matrix M is introduced.[‡‡‡‡] It is assumed to be a constant. Further, we limit our considerations to the case where one may assume a single frequency and omit the ϵ_{jk}'s, i.e., the situation treated in Sec. 9.

Combining (8.16), (8.18), and (9.8) results in

$$\alpha(\nu)=bN\frac{4\pi^2}{3\hbar c}|\langle\varphi'|e\mathbf{r}|\varphi\rangle|^2\nu G(\nu)$$

$$=K'M^2\nu\frac{1}{2\pi}\int_{-\infty}^{\infty}e^{-i(\nu-\nu_{ug})t}$$

$$\times\exp\{-S[\coth\tfrac{1}{2}\beta-i\sin\omega t-\coth\tfrac{1}{2}\beta\cos\omega t]\}dt,\quad(17.1)$$

where

$$K'=4\pi^2bN/3\hbar c\quad(17.1a)$$

and

$$M=\langle\varphi'|e\mathbf{r}|\varphi\rangle.\quad(17.1b)$$

Since our interest is in the moments of the distribution, we assume that the absorption is a series of delta functions.

Taking the Fourier transformation of $\alpha(\nu)/\nu$, one arrives at

$$\int_{-\infty}^{\infty}[\alpha(\nu)/\nu]e^{i\nu t}d\nu=K'M^2e^{i\nu_{ug}t}$$

$$\times\exp\{-S[\coth\tfrac{1}{2}\beta-i\sin\omega t-\coth\tfrac{1}{2}\beta\cos\omega t]\}.\quad(17.2)$$

From this it follows that

$$M_0=(\hbar/i)\left\{(\partial/\partial t)\int_{\infty}^{\infty}[\alpha(\nu)/\nu]e^{i\nu t}d\nu\right\}_{t=0}$$

$$=\hbar K'M^2\{\nu_{ug}+S\omega\}=K'M^2\Delta\epsilon=K\hbar\bar{f},\quad(17.3)$$

where

$$\bar{f}=2m\bar{\nu}M^2/3e^2\hbar\quad(17.3a)$$

and

$$\bar{\nu}=\Delta\epsilon/\hbar.\quad(17.3b)$$

Use has been made of (10.1a) and (10.14). (17.3) should be compared to (10.9). Further,

$$M_1=-\hbar^2\{(\partial^2/\partial t^2)\textstyle\int_{-\infty}^{\infty}[\alpha(\nu)/\nu]e^{i\nu t}d\nu\}_{t=0}$$

$$=K'M^2[(\Delta\epsilon)^2+\hbar^2\omega^2S\coth\tfrac{1}{2}\beta]$$

$$=K'M^2\Delta\epsilon[\Delta\epsilon+(\hbar^2\omega^2/\Delta\epsilon)S\coth\tfrac{1}{2}\beta]\quad(17.4)$$

and

$$M_2=-(\hbar^3/i)\{\partial^3/\partial t^3)\textstyle\int_{-\infty}^{\infty}[\alpha(\nu)/\nu]e^{i\nu t}d\nu\}_{t=0}$$

$$=K'M^2\Delta\epsilon[(\Delta\epsilon)^2+3\omega^2\hbar^2S\coth\tfrac{1}{2}\beta$$

$$+(\omega^3\hbar^3/\Delta\epsilon)S].\quad(17.5)$$

Further,

$$\bar{\epsilon}=\Delta\epsilon+(\hbar^2\omega^2/\Delta\epsilon)S\coth\tfrac{1}{2}\beta\quad(17.6)$$

and

$$m^2=\omega^2\hbar^2S\{\coth\tfrac{1}{2}\beta+(\omega\hbar/\Delta\epsilon)$$

$$-[\hbar^2\omega^2/(\Delta\epsilon)^2]S\coth^2\tfrac{1}{2}\beta\}.\quad(17.7)$$

Equation (17.6) shows that $\bar{\epsilon}$ shifts to the *violet* with rising temperatures. The shift is very small, since $\hbar^2\omega^2S/\Delta\epsilon$ is of the order of 0.0015 ev. If $\hbar\omega$ were 0.08 ev and $S\approx30$ this term would be observable. This might occur in LiF if the transverse optical mode were important for the interaction. m^2 now has a constant term and a term proportional to $\coth^2\tfrac{1}{2}\beta$. The negative sign on this term means that m^2 can be negative at *very* high temperatures. This anomalous situation arises from the mathematical formulation and has nothing to do with actual emission. By returning to (17.1) we see that $\alpha(\nu)<0$ if $\nu<0$. Since the mathematical techniques require integration from $-\infty$ to $+\infty$, the integral $\int_{-\infty}^{\infty}(\nu-\bar{\nu})^2\nu G(\nu)d\nu$ can be negative in spite of the fact that $(\nu-\bar{\nu})^2>0$. The author expects that both additional terms in (17.7) are very small and will not be detected experimentally.

The form (17.7) is not valid at extremely high temperatures, say 5000°K, if $(\hbar\omega)^2S/(\Delta\epsilon)^2$ is of the order of 10^{-3}. For the F center in KCl this term is of the order of 8×10^{-4}, and our interests are limited to temperatures below 600°K. The above calculations are most probably valid under these conditions. They indicate that the assumption that f is independent of ν does not have an important influence on the moments. In the language of Dexter (D1, p. 392), we have shown when the "narrow-band approximation" is valid.

(b) Oscillator Strength Depends on the q's

In the case where $f^{\frac{1}{2}}$ depends on the normal modes, the solution is straightforward but extremely laborious. To simplify the problem somewhat the CC model will be used, thus $f^{\frac{1}{2}}$ is taken in the form

$$f^{\frac{1}{2}}=f_0^{\frac{1}{2}}+f_1^{\frac{1}{2}}q.\quad(17.8)$$

Equation (17.8) is a possible assumption, and it is

[‡‡‡‡] For simplicity of notation M is considered to be a real scalar.

made without any profound theoretical justification. In (17.8) q is the coordinate associated with the ground state. The normal mode for the excited state is taken in the form $q-\Delta q=Q$. Further, we again assume that the ϵ_{jk}'s are very small so that the frequencies in both states are equal. As before, $f^{\frac{1}{2}}$ is taken as real; further, our considerations will be limited to terms in $f_1^{\frac{1}{2}}$. Equation (10.6) cannot be used, and we require some more complex equations given by Lax (L1), namely,

$$M_0=\hbar K\ \mathrm{Av}\{\chi|f|\chi\} \tag{17.9}$$

$$M_1=\hbar K\ \mathrm{Av}\{\chi|f^{\frac{1}{2}}H_u f^{\frac{1}{2}}-fH_g|\chi\} \tag{17.10}$$

and

$$M_2=\hbar K\ \mathrm{Av}\{\chi|f^{\frac{1}{2}}H_u^2 f^{\frac{1}{2}} -2f^{\frac{1}{2}}H_u f^{\frac{1}{2}}H_g+fH_g^2|\chi\}. \tag{17.11}$$

Equation (17.10) is equivalent to (10.12) provided

$$\{\chi|H_uH_g|\chi\}=\{\chi|H_gH_u|\chi\} \tag{17.12}$$

when f is independent of q.

To establish (17.12) we require some of the properties of the χ's. One may show (M7, p. 121 and 358)§§§§

$$(\partial/\partial q)\chi_v=(\omega/\hbar)^{\frac{1}{2}}\{(\tfrac{1}{2}v)^{\frac{1}{2}}\chi_{v-1}-[\tfrac{1}{2}(v+1)]^{\frac{1}{2}}\chi_{v+1}\} \tag{17.13}$$

$$q\chi_v=(\hbar/\omega)^{\frac{1}{2}}\{[\tfrac{1}{2}(v+1)]^{\frac{1}{2}}\chi_{v+1}+(v/2)^{\frac{1}{2}}\chi_{v-1}\}. \tag{17.14}$$

Hence

$$\{\chi|q(\partial/\partial q)|\chi\}=-\tfrac{1}{2} \tag{17.15}$$

and

$$\{\chi|TV_{u,g}|\chi\}=\{\chi|V_{u,g}T|\chi\}. \tag{17.16}$$

To establish (17.16) we have used (3.26) but placed no restriction on the v's; hence, (17.16) applies to the case considered in Sec. 10 and is the justification for Eq. (10.12). A similar argument has not been found for terms in $(H_u-H_g)^3$, and the technique of Sec. 10 requires lengthy and complex algebra.

Returning to (17.8), we note from (17.13) and (17.14) that our interest is limited to even terms of the q's, i.e., such as q^2 or $q(\partial/\partial q)$, not q^3 or $\partial/\partial q$. Hence, substituting (17.8) in (17.9), one obtains

$$M_0=\hbar K f_0. \tag{17.17}$$

Had terms in f_1 been included, we would have found that M_0 is temperature *dependent*. Now, substituting into (17.10), we obtain

$$M_1=\hbar K\ \mathrm{Av}\{\chi|f_0(V_u-V_g) -2f_0^{\frac{1}{2}}f_1^{\frac{1}{2}}\omega^2(\Delta q)q^2|\chi\} \tag{17.18}$$

$$=\hbar K(f_0\Delta\epsilon-\omega\hbar\Delta q f_0^{\frac{1}{2}}f_1^{\frac{1}{2}}\coth\tfrac{1}{2}\beta) \tag{17.19}$$

$$=\hbar K f_0\left\{\Delta\epsilon-\omega\hbar\left[\frac{M(d)-M(a)}{M(a)}\right]\coth\tfrac{1}{2}\beta\right\}. \tag{17.19a}$$

$M(a)$ and $M(d)$ are dipole moments at positions (a) and (d) of Fig. 2. The ratio $[M(d)-M(a)]/M(a)$ must be of the order of 0.1 or much less, probably much less. The second term of (17.19a) cannot possibly be larger than 0.001, and we would not expect to detect it experimentally. Further,

$$M_2=\hbar K\ \mathrm{Av}\{\chi|f_0(V_u-V_g)^2+f_0^{\frac{1}{2}}f_1^{\frac{1}{2}}[TV_uq+V_uTq +qTV_u-3qV_uT+2q(V_u-V_g)^2]|\chi\}. \tag{17.20}$$

Since

$$\{\chi|TV_uq|\chi\}=\{\chi|qV_uT|\chi\} \tag{17.21a}$$

$$\{\chi|V_uTq|\chi\}=\{\chi|qTV_u|\chi\} =\{\chi|qV_uT|\chi\}-(\hbar^2/2)\omega^2\Delta q, \tag{17.21b}$$

we have

$$M_2=\hbar K\ \mathrm{Av}\{\chi|(V_u-V_g)^2f_0+f_0^{\frac{1}{2}}f_1^{\frac{1}{2}}[2q(V_u-V_g)^2 -\hbar^2\omega^2\Delta q]|\chi\}. \tag{17.22}$$

The third term gives rise to a temperature independent factor in m^2. Taking the indicated average in (17.22) results in

$$M_2=\hbar K\{f_0[(\Delta\epsilon)^2+\hbar^2\omega^2S\coth\tfrac{1}{2}\beta] -\Delta q f_0^{\frac{1}{2}}f_1^{\frac{1}{2}}[2\Delta\epsilon\hbar\omega\coth\tfrac{1}{2}\beta+\hbar^2\omega^2]\}. \tag{17.23}$$

Returning to (7.3) we obtain

$$m^2=\hbar^2\omega^2[S\coth\tfrac{1}{2}\beta-\Delta q(f_1^{\frac{1}{2}}/f_0^{\frac{1}{2}})]. \tag{17.24}$$

To estimate the magnitude of the second term we again use Fig. 2. From the definitions of the f's and Δq one obtains

$$\Delta q f_1^{\frac{1}{2}}/f_0^{\frac{1}{2}}=[M(d)-M(a)]/M(a). \tag{17.25}$$

The maximum correction term that one may expect in (17.24) is 0.1. Such small values could barely be detected experimentally (Sec. 10). Meyer (M8) suggested that this term equals −10. Such large values cannot be explained readily by the theory.

The conclusion is rather straightforward. The assumptions used in arriving at (8.18) are most probably oversimplified. However, they do not produce major changes in the moments of the distribution or in the shapes. Some corrections to the moments have been worked out here. They are certainly too small to be measured, and the author cannot envisage any theoretical calculation which will be sufficiently accurate to determine them. One may show experimentally, however, that M_3 has a complex temperature dependence (K4). The theoretical reason for this is at present unknown. The author believes this will come out of a more realistic model.

BIBLIOGRAPHY

A1. M. Abraham and R. Becker, *The Classical Theory of Electricity and Magnetism* (Blackie and Son, Ltd., London, 1950).

B1. R. L. Bjork, Phys. Rev. **105**, 456 (1957).

B2. M. Born and K. Huang, *Dynamical Theory of Crystal Lattices* (Clarendon Press, Oxford, 1954).

---

§§§§ The subscript is the vibrational quantum number.

B3. M. Born and J. Oppenheimer, Ann. phys. **84**, 457 (1927).
B4. M. A. Bredig, Z. Physik **46**, 73 (1927).
B5. E. Burstein and J. J. Oberly, Natl. Bur. Standards (U.S.) Circ. No. 519, 285 (1952).
C1. T. G. Castner and W. Kanzig, J. Phys. Chem. Solids **3**, 178 (1957).
C2. D. W. Compton (private communication).
C3. D. W. Compton and C. C. Klick, Phys. Rev. **110**, 349 (1958).
D1. D. L. Dexter in *Solid State Physics*, edited by F. Seitz and D. Turnbull (Academic Press, Inc., New York, 1958), Vol. 6.
D2. W. H. Duerig and J. J. Markham, Phys. Rev. **88**, 1043 (1952).
D3. C. Z. van Doorn and Y. Haven, Philips Research Repts. **11**, 479 (1956).
D4. D. Dutton and R. Maurer, Phys. Rev. **90**, 126 (1953).
F1. H. Frölich, Proc. Roy. Soc. (London) **A160**, 230 (1937).
F2. H. Frölich, Advances in Phys. **3**, 325 (1954).
F3. Fröhlich, Pelzer, and Zienau, Phil. Mag. **41**, 221 (1950).
H1. H. Haken, Z. Physik, **135**, 408 (1953).
H2. A. Haug, Z. Physik **146**, 75 (1956).
H3. W. Heitler, *The Quantum Theory of Radiation* (Clarendon Press, Oxford, 1954), third edition.
H3a. F. A. Henglein, Z. physik Chem. **115**, 91 (1925).
H4. K. Huang, Proc. Roy. Soc. (London) **A208**, 352 (1951).
H5. K. Huang and A. Rhys, Proc. Roy. Soc. (London) **A204**, 406 (1950).
I1. H. F. Ivey, Phys. Rev. **72**, 341 (1947).
J1. H. Jeffreys and B. S. Jeffreys, *Methods of Mathematical Physics* (University Press, Cambridge, England, 1946).
K1. H. Kanzaki, Phys. Rev. **110**, 1063 (1958).
K2. C. C. Klick, Phys. Rev. **85**, 154 (1952).
K2a. C. C. Klick and J. H. Schulman, in *Solid State Physics*, edited by F. Seitz and D. Turnbull (Academic Press, Inc., New York, 1957), Vol. 5.
K3. J. D. Konitzer and J. J. Markham, Phys. Rev. **107**, 685 (1957).
K4. J. D. Konitzer and J. J. Markham (to be submitted).
K5. M. A. Krivoglaz and S. I. Pekar, Trudy Inst. Fiz., Akad. Nauk Ukr. S. S. R. **4**, 37 (1953) (in Russian).
K6. R. Kubo and Y. Toyozawa, Progr. Theoret. Phys. (Kyoto) **13**, 160 (1955).
L1. M. Lax, J. Chem. Phys. **20**, 1752 (1952).
L2. M. Lax, *Photoconductivity Conference*, edited by R. G. Breckenridge (John Wiley and Sons, Inc., New York, 1956), p. 111.
L2a. M. Lax and E. Burstein, Phys. Rev. **100**, 592 (1955).
L3. K. Lonsdale, *Crystals and X-rays* (G. Bell and Sons, London, 1948).
M1. Mador, Markham, and Platt, Phys. Rev. **91**, 1277 (1953).
M2. Maradudin, Mazur, Montroll, and Weiss, Revs. Modern Phys. **30**, 175 (1958).
M3. J. J. Markham, J. Chem. Phys. **16**, 580 (1948).
M4. J. J. Markham, Phys. Rev. **103**, 588 (1956).
M5. J. J. Markham and J. D. Konitzer, J. Chem. Phys. **29**, 673 (1958); **30**, 328 (1959).
M6. J. J. Markham and F. Seitz, Phys. Rev. **74**, 1014 (1948).
M7. H. Margenau and G. M. Murphy, *The Mathematics of Physics and Chemistry* (D. Van Nostrand and Company, Inc., Princeton, New Jersey, 1956), second edition.
M8. H. J. G. Meyer, Physica **21**, 253 (1955).
M9. H. J. G. Meyer, Halbleitprobleme **3**, 230 (1956).
M10. E. Mollwo, Z. Physik **85**, 56 (1933).
M11. J. P. Molnar, "The absorption spectra of trapped electrons in alkali halide crystals," thesis, Massachusetts Institute of Technology, 1940 (unpublished).
M12. N. F. Mott and R. W. Gurney, *Electronic Processes in Ionic Crystals* (Clarendon Press, Oxford, 1948).
M13. T. Muto, Progr. Theoret. Phys. (Kyoto) **4**, 181 (1949).
O1. R. C. O'Rourke, Phys. Rev. **91**, 265 (1953).
P1. S. I. Pekar, J. Exptl. Theoret. Phys. (U.S.S.R.) **20**, 510 (1950), translated by Professor B. Goodman.
P2. S. I. Pekar, J. Exptl. and Theoret. Phys. (U.S.S.R.) **22**, 641 (1952), translated by A. Pingell, Naval Research Laboratory.
P3. S. I. Pekar, Uspekhi Fiz. Nauk **50**, 197 (1953), translated by M. F. Friedman of Newtonville, Massachusetts.
P4. S. I. Pekar, *Untersuchungen über die Elektronentheorie der Kristalle* (Akademische-Verlagsgesellschaft, Berlin, 1954).
P5. P. Pringsheim, Z. Physik **136**, 573 (1954).
R1. G. A. Russell and C. C. Klick, Phys. Rev. **101**, 1473 (1956).
S1. F. Seitz, Revs. Modern Phys. **26**, 7 (1954).
S2. F. Seitz, *The Modern Theory of Solids* (McGraw-Hill Book Company, Inc., New York, 1940).
S3. J. H. Simpson, Proc. Roy. Soc. (London) **A197**, 266 (1949).
S4. J. C. Slater, *Quantum Theory of Matter* (McGraw-Hill Book Company, Inc., New York, 1951).
S5. J. C. Slater, *Introduction to Chemical Physics* (McGraw-Hill Book Company, Inc., New York, 1939).
S6. W. A. Smith, "Energy level calculations for F centers and positive ions in alkali halides," Knolls Atomic Power Laboratory (Rept. KAPL-1720, April 1, 1957).
V1. J. H. Van Vleck, *The Theory of Electric and Magnetic Susceptibilities* (Clarendon Press, Oxford, 1932).
V2. H. D. Vasileff, Phys. Rev. **96**, 603 (1954).
W1. G. N. Watson, J. London Math. Soc. **8**, 194 (1933).
W2. F. E. Williams, J. Chem. Phys. **19**, 457 (1951).
W3. F. E. Williams and M. H. Hebb, Phys. Rev. **84**, 1181 (1951).
W4. A. H. Wilson, *The Theory of Metals* (University Press, Cambridge, England, 1953).